



**HAL**  
open science

## **BCL2-ASSOCIATED ATHANOGENE4 Regulates the KAT1 Potassium Channel and Controls Stomatal Movement**

Antonella Locascio, Maria Carmen Marqués, Guillermo García-Martínez, Claire Corratgé-Faillie, Nuria Andrés-Colás, Lourdes Rubio, José Antonio Fernández, Anne-Aliénor Véry, José Miguel Mulet, Lynne Yenush

► **To cite this version:**

Antonella Locascio, Maria Carmen Marqués, Guillermo García-Martínez, Claire Corratgé-Faillie, Nuria Andrés-Colás, et al.. BCL2-ASSOCIATED ATHANOGENE4 Regulates the KAT1 Potassium Channel and Controls Stomatal Movement. *Plant Physiology*, 2019, 181 (3), pp.1277-1294. 10.1104/pp.19.00224 . hal-02349953

**HAL Id: hal-02349953**

**<https://hal.science/hal-02349953>**

Submitted on 10 Aug 2022

**HAL** is a multi-disciplinary open access archive for the deposit and dissemination of scientific research documents, whether they are published or not. The documents may come from teaching and research institutions in France or abroad, or from public or private research centers.

L'archive ouverte pluridisciplinaire **HAL**, est destinée au dépôt et à la diffusion de documents scientifiques de niveau recherche, publiés ou non, émanant des établissements d'enseignement et de recherche français ou étrangers, des laboratoires publics ou privés.

1 **Short title: AtBAG4 is a KAT1 potassium channel regulator**

2 \*Author for Contact details

3 Lynne Yenush

4 Instituto de Biología Molecular y Celular de Plantas, Universitat Politècnica de Valencia-

5 Consejo Superior de Investigaciones Científicas, 46022 Valencia, SPAIN

6 +34963879375

7 **Title: BCL2-ASSOCIATED ATHANOGENE4 Regulates the KAT1 Potassium Channel and**  
8 **Controls Stomatal Movement**

9

10 **Author names and affiliations:** Antonella Locascio<sup>1</sup>, M<sup>a</sup> Carmen Marqués<sup>1</sup>, Guillermo  
11 García-Martínez<sup>1</sup>, Claire Corratgé-Faillie<sup>2</sup>, Nuria Andrés-Colás<sup>1</sup>, Lourdes Rubio<sup>3</sup>, José  
12 Antonio Fernández<sup>3</sup>, Anne-Aliénor Véry<sup>2</sup>, José Miguel Mulet<sup>1</sup>, Lynne Yenush<sup>1\*</sup>

13 <sup>1</sup> Instituto de Biología Molecular y Celular de Plantas, Universitat Politècnica de Valencia-  
14 Consejo Superior de Investigaciones Científicas, 46022 Valencia, SPAIN

15

16 <sup>2</sup> Biochimie et Physiologie Moléculaire des Plantes, Univ Montpellier, CNRS, INRA, SupAgro  
17 Montpellier, Campus SupAgro-INRA, 34060 Montpellier Cedex 2, France

18

19 <sup>3</sup> Facultad de Ciencias. Universidad de Málaga. Campus de Teatinos S/N 29010 Málaga, SPAIN

20

21

22 **One Sentence summary:** The evolutionarily conserved Arabidopsis protein BAG4  
23 regulates the KAT1 potassium channel and stomatal movement, and is a possible  
24 target for development of plants with increased water use efficiency.

25

26 **Author Contributions:** AL, MM, GG-M, NA-C, CC-F and LY performed the experiments;  
27 LY and JMM designed and supervised the project; LY, JMM, AL, LR, A-AV, JAF and CC-F  
28 participated in the experimental design and writing of the manuscript.

29

30 **Funding Information:** This work was supported by the Spanish Ministry of Economy  
31 and Competitiveness (BIO201677776-P and BIO2016-81957-REDT) and the Valencian  
32 Government (AICO/2018/300).

33

34 **Email address for Author for Contact:** [lynne@ibmcp.upv.es](mailto:lynne@ibmcp.upv.es)

35

36

37

38

39

40 **Abstract**

41 Potassium (K<sup>+</sup>) is a key monovalent cation necessary for multiple aspects of cell growth  
42 and survival. In plants, this cation also plays a key role in the control of stomatal  
43 movement. KAT1 and its homolog KAT2 are the main inward rectifying channels  
44 present in guard cells, mediating K<sup>+</sup> influx into these cells, resulting in stomatal  
45 opening. To gain further insight into the regulation of these channels, we performed a  
46 split-ubiquitin protein-protein interaction screen searching for KAT1 interactors in  
47 *Arabidopsis* (*Arabidopsis thaliana*). We characterized one of these candidates, BCL2-  
48 ASSOCIATED ATHANOGENE4 (BAG4), in detail using biochemical and genetic  
49 approaches to confirm this interaction and its effect on KAT1 activity. We show that  
50 BAG4 improves KAT1-mediated K<sup>+</sup> transport in two heterologous systems and provide  
51 evidence that in plants, BAG4 interacts with KAT1 and favors the arrival of KAT1 at the  
52 plasma membrane. Importantly, lines lacking or overexpressing the *BAG4* gene show  
53 altered KAT1 plasma membrane accumulation and alterations in stomatal movement.  
54 Our data allowed us to identify a KAT1 regulator and define a potential target for the  
55 plant BAG family. The identification of physiologically relevant regulators of K<sup>+</sup>  
56 channels will aid in the design of approaches that may impact drought tolerance and  
57 pathogen susceptibility.

58

59 **Key words:** Arabidopsis, BAG4, K<sup>+</sup> channel regulator, KAT1, KAT2, stomata regulation

60 **Introduction**

61 Ion homeostasis is a dynamic process essential for the normal functioning of any  
62 organism. Some minerals are required for biological processes, but their excess or  
63 deficiency is deleterious. In addition, cells must discriminate between the  
64 physiologically relevant ions and the toxic ions that may be chemically similar. For this  
65 reason, all living organisms have developed efficient systems to capture and store ions  
66 and complex mechanisms to maintain homeostatic concentrations. In plants, ion  
67 homeostasis must provide the environment required to maintain all internal  
68 processes, prevent toxicity and enable the response to environmental changes using  
69 the minerals present in the soil.

70 Potassium is a key monovalent cation necessary for many aspects of growth and  
71 survival, among them, compensation of the negative charges generated in processes  
72 such as glycolysis, the maintenance of electroneutrality, turgor pressure and cell  
73 volume, phloem loading, enzymatic activity, protein synthesis and the establishment of  
74 proper membrane potential and an adequate intracellular pH (Rodríguez-Navarro,  
75 2000).

76 In plant cells, potassium accumulates to relatively high concentrations in the plant cell  
77 cytosol (about 100 mM) and in variable amounts in the vacuole (10-200 mM,  
78 depending on the tissue and the environmental conditions), while other cations such  
79 as sodium must be excluded to avoid toxicity (Pardo and Quintero, 2002). Potassium  
80 homeostasis is essential for optimal water use efficiency, as potassium currents  
81 participate in stomatal movement. Stomatal opening depends on potassium and anion  
82 uptake coupled to increased proton efflux, while stomatal closing depends on  
83 potassium and anion efflux (Lawson and Blatt, 2014). Understanding the molecular  
84 mechanisms underlying potassium regulation in guard cells can provide valuable  
85 information with applications to the development of new varieties of drought resistant  
86 crops. In response to elevated CO<sub>2</sub>, drought may be among the main threats to world  
87 food production because of its dramatic impact on agricultural productivity. Optimizing  
88 water use efficiency of crops by improving the potassium regulation in the guard cell,

89 and therefore improving transpiration regulation, can directly affect food production  
90 under adverse conditions (Wang et al., 2014).

91 In the model plant *Arabidopsis thaliana*, there are three different families of plasma  
92 membrane potassium transport systems: the CPA2 subfamily including CHX and KEA  
93 H<sup>+</sup>/K<sup>+</sup> antiporters (Mäser et al., 2001), the HAK/KUP/KT K<sup>+</sup> transporters (Gierth and  
94 Mäser, 2007), and the Shaker-type K<sup>+</sup> channels (Véry and Sentenac, 2003). The third  
95 family, Shaker channels, is present in animals, plants, yeast and bacteria. The genome  
96 of *Arabidopsis* contains 9 members that are classified into 5 different groups  
97 depending on their phylogeny and functional aspects (Pilot et al., 2003). Groups 1 and  
98 2 contain 4 inward rectifying channels (AKT1, AKT6, KAT1 and KAT2, respectively),  
99 while group 3 contains a weak inward rectifier (AKT2). Group 4 contains a "Silent"  
100 channel (KC1) and group 5 consists of two outwardly rectifying channels (GORK and  
101 SKOR). This family of voltage-dependent channels selective for potassium is  
102 responsible for the K<sup>+</sup> conductance in the plasma membrane in most cell types. Based  
103 on the structural data obtained for bacterial and mammalian Shaker channels, it has  
104 been proposed that this family adopts a homo- or hetero-tetrameric structure that  
105 forms the potassium pore (Jiang et al., 2003; Long et al., 2005). For example, AKT1 has  
106 been proposed to form functional channels with KC1 and KAT2, while KAT1 and KAT2  
107 can associate with each other and also with KC1 (and AKT2 in the case of KAT2)  
108 (Lebaudy et al., 2010; Jeanguenin et al., 2011). KC1 is considered a "silent" channel  
109 since it is only able to induce currents when it is part of heterotetramers (Dreyer et al.,  
110 1997; Duby et al., 2008; Jeanguenin et al., 2011). It is considered that this multiplicity  
111 in the composition of subunits confers different properties to the channel and this  
112 would be a reflection of different physiological functions (Ivashikina et al., 2001;  
113 Xicluna et al., 2007; Jeanguenin et al., 2011).

114 Two members of the Shaker family, KAT1 and KAT2 are major contributors to  
115 potassium influxes in guard cells (Nakamura et al., 1995; Szyroki et al., 2001; Lebaudy  
116 et al., 2008). As potassium homeostasis contributes to the regulation of stomatal  
117 movement, this process requires tight regulation, which allows fast activation and  
118 inactivation, to prevent excessive water loss, specifically under drought or saline  
119 conditions (Lebaudy et al., 2008). Therefore, the identification and characterization of

120 the proteins interacting with the KAT1 potassium channel may provide new insights  
121 into potassium homeostasis regulation and new ways to develop drought tolerant  
122 plants.

123 KAT1 is considered the prototype of inward rectifying potassium channels and plays an  
124 important role in potassium fluxes in the guard cell, as mentioned above (Anderson et  
125 al., 1992; Schachtman et al., 1992; Nakamura et al., 1995). Several proteins have been  
126 implicated in KAT1 regulation. For example, it has been described that fusicoccin can  
127 stabilize the interaction of KAT1 with 14-3-3 proteins and activate its transport activity  
128 (Saponaro et al., 2017), but the underlying mechanism of this regulation at the level of  
129 protein-protein interaction remains largely unexplored. Previous studies have shown  
130 that both the Ost1 (SnRK2.6) and the CPK13 kinases can phosphorylate KAT1, although  
131 the molecular mechanism by which these phosphorylation events regulate the channel  
132 are as yet undefined (Sato et al., 2009; Ronzier et al., 2014). In addition, work from the  
133 Blatt laboratory has shown that VAMP721 and SYP121 are important for KAT1  
134 trafficking and gating of the channel (Sutter et al., 2006; Eisenach et al., 2012; Zhang et  
135 al., 2015; Zhang et al., 2017; Lefoulon et al., 2018). As these channels play an  
136 instrumental role in stomatal movement, their regulation is likely to be complex,  
137 involving several different classes of regulatory molecules.

138 In the present report, we used a split-ubiquitin approach to identify proteins  
139 interacting with KAT1. We found that the BCL2-Associated Athanogene (BAG) 4 protein  
140 interacts with KAT1. BAG4 is a member of an evolutionarily conserved family defined  
141 by the presence of the BAG domain. This domain is approximately 110-125 amino acids  
142 long and is composed of three antiparallel  $\alpha$  helices of 30-40 amino acids (Takayama  
143 and Reed, 2001). BAG family proteins have been extensively studied in mammalian  
144 systems where they have been shown to regulate several processes in many cases by  
145 recruiting co-chaperones and different chaperone systems, including the Heat shock  
146 protein 70 (Hsp70), which binds to helices 2 and 3 of the BAG domain (Takayama and  
147 Reed, 2001; Kabbage and Dickman, 2008). In plants, BAG proteins have been related to  
148 processes such as the unfolded protein response, pathogen resistance and abiotic  
149 stress and have been shown to conserve the ability to bind to Hsp70 (Doukhanina et  
150 al., 2006; Williams et al., 2010; Kabbage et al., 2016), although the molecular

151 mechanisms underlying their function are largely undefined. More specifically,  
152 overexpression of BAG4 is able to increase salinity tolerance in Arabidopsis and rice  
153 (Doukhanina et al., 2006; Hoang et al., 2015), and BAG1 and BAG6 have been  
154 implicated in the proteasomal degradation of plastid proteins and fungal resistance,  
155 respectively (Kabbage et al., 2016; Lee et al., 2016). In this report, we show that BAG4  
156 expression increases KAT1 activity in both yeast and *Xenopus* oocytes. Moreover, we  
157 have confirmed the KAT1-BAG4 interaction in plants and provide evidence that BAG4  
158 plays a role in the arrival of KAT1 at the plasma membrane in both gain- and loss-of-  
159 function experiments. In addition, mutants lacking or overexpressing the *BAG4* gene  
160 present alterations in stomatal opening dynamics, consistent with a physiological role  
161 in modulating potassium fluxes. Taken together, our data suggest that in plants BAG4  
162 acts as a KAT1 regulator. Our work uncovers an important potential client for the plant  
163 BAG protein family.

164 **Results**

165 In order to gain further insight into the post-translational regulation of the KAT1  
166 inward rectifying potassium channel, we carried out a high-throughput screening for  
167 physical interactors using the Split-ubiquitin yeast two-hybrid assay with an  
168 Arabidopsis cDNA library, as described in Materials and Methods. Previous reports  
169 have shown that KAT1 interactions can be detected using this method (Obrdlik et al.,  
170 2004). Using this approach, we identified BAG4 as a KAT1 interacting protein.

171 As a first step in the characterization of this interaction, we carried out a functional  
172 complementation assay in yeast for selected candidates. We co-transformed KAT1  
173 with BAG4 and two other candidate proteins into a yeast strain lacking its endogenous  
174 high affinity potassium transporters (Trk1 and Trk2). This strain grows very poorly in  
175 media with limiting amounts of potassium (12  $\mu$ M) (Navarrete et al., 2010). However,  
176 KAT1 expression functionally complements this phenotype. The plasmid containing the  
177 *KAT1* sequence is under control of the *MET25* promoter and in the presence of 0.75  
178 mg/ml methionine the expression of *KAT1* is reduced to low levels (Mumberg et al.,  
179 1994), providing a sensitive system to study KAT1 activity. In order to determine  
180 whether BAG4 could functionally regulate KAT1, we performed growth assays in liquid  
181 media under three conditions: 1) low KAT1 expression (methionine supplementation)  
182 and low potassium (no KCl supplementation), 2) low KAT1 expression and high  
183 potassium (50 mM KCl), and 3) high KAT1 expression and low potassium. As shown in  
184 Fig. 1, co-expression of BAG4 with KAT1 improved growth under limiting potassium  
185 conditions, whereas two other Arabidopsis proteins recovered in the screening, (PPI1  
186 (Proton pump interacting protein 1) and RPT2 (Root phototropism 2)), had no  
187 functional effect in this assay. Correct expression of the proteins was confirmed by  
188 immunodetection (Fig. 1). As observed, both BAG4 and PPI1 accumulated to similar  
189 levels, whereas RPT2 accumulated to lower levels in yeast. This result is consistent  
190 with BAG4 improving KAT1 activity in this heterologous system. Based on this  
191 phenotype, BAG4 was selected for further analysis. We next wanted to confirm that  
192 the increase in growth in this assay was not due to increased expression of the KAT1  
193 protein upon BAG4 overexpression. For this, we determined the levels of KAT1 in 6  
194 control strains and 7 strains co-expressing BAG4. As shown in Figure 1, we observed



195 no change in KAT1 protein levels, suggesting that the effect of BAG4 is not due to  
196 increased accumulation of KAT1, and so discards mechanisms based on transcriptional  
197 regulation and protein turnover in this model system.

198 BAG4 belongs to a seven member family of proteins all containing a BAG domain  
199 (Doukhanina et al., 2006). BAG1 and BAG7 have a domain structure similar to BAG4  
200 and so were chosen for further analysis. Using the yeast assays described above, we  
201 compared both the interaction and the functional complementation between BAG  
202 family members. Since the original BAG4 clone recovered from the screening had a 13  
203 amino acid N-terminal truncation, we cloned the full-length *BAG4* gene and included it  
204 in these assays. As observed in the split-ubiquitin protein-protein interaction assay  
205 shown in Figure 2, we observed the strongest interaction between KAT1 and the BAG4  
206 isoforms, as judged by the growth in selective media and the X-gal plate assay. A  
207 moderate interaction was observed for BAG1, whereas the interaction between KAT1  
208 and BAG7 was very weak. The data presented in Figure 2 confirms the proper  
209 expression of each of the proteins. The same pattern of relative KAT1-BAG protein  
210 interaction (BAG4>BAG1>>BAG7) was observed in the functional complementation  
211 assay shown in Figure 2. The combinations between KAT1 and both versions of BAG4  
212 show the highest growth in low potassium medium when KAT1 is limiting (black bars).  
213 Some growth is detected under these conditions upon co-expression of BAG1, but in  
214 the presence of BAG7 the level of growth is the same as the control. Thus, we provide  
215 evidence for some level of specificity between KAT1 and BAG family members, lending  
216 further support to the possible physiological relevance of the KAT1-BAG4 interaction.

217 In order to confirm that the observed improvement in growth of the KAT1\_BAG4 strain  
218 is due to improved potassium uptake, we analyzed potassium uptake using K<sup>+</sup>-specific  
219 electrodes (see Materials and Methods for a complete description). As shown in Figure  
220 3, co-expression of BAG4 increased both the total amount and the initial rate of  
221 potassium uptake from the media. As an internal control, we measured the  
222 acidification of the media (due to the H<sup>+</sup>-ATPase activity) and, as expected, observed  
223 no changes in the presence or absence of BAG4 (Fig. 3). These experiments strongly  
224 suggest that BAG4 favors KAT1 potassium transport activity, at least in yeast.

225 *Xenopus* oocytes have been extensively used to characterize potassium channels from  
226 many organisms. We studied the effect of BAG4 co-expression on KAT1-mediated  
227 currents in this model system. We observed an increase in KAT1 channel activity one  
228 day after cRNA injection into the oocytes (Fig. 4 and Supplemental Fig. S1). At later  
229 times (from Day 2), when reaching steady-state expression level, no differences in the  
230 currents were observed (Supplemental Fig. S1). KAT1 current increase upon BAG4 co-  
231 expression one day after oocyte injection was 50% to 100% in the different  
232 experiments at all membrane voltages (Fig. 4 and Supplemental Fig. S1). No shift in  
233 KAT1 voltage-dependence was observed under co-expression (Fig. 4). One  
234 interpretation of these results contends that BAG4 co-expression favors the targeting  
235 of active KAT1 channels at the oocyte cell membrane, consistent with what is observed  
236 in the experiments described above in yeast.

237 We next wanted to confirm that the interaction between BAG4 and KAT1 also takes  
238 place in plants. To this end, we performed both Bimolecular Fluorescence  
239 Complementation (BiFC) and co-immunoprecipitation assays in *Nicotiana benthamiana*  
240 infiltrated with *Agrobacterium tumefaciens* containing the appropriate plasmids. As a  
241 positive control, we used the KAT1-KAT1 interaction (Fig. 5), observing a uniform  
242 fluorescent signal at the plasma membrane. By contrast, we observed a punctate  
243 signal corresponding to the KAT1-BAG4 interaction but observed no signal for the  
244 corresponding control experiments (Fig. 5). In addition, to add experimental support  
245 for this interaction in plants, we performed co-immunoprecipitation experiments upon  
246 transient expression in *N. benthamiana*. We were able to efficiently recover BAG4  
247 upon KAT1 immunoprecipitation performed in protein extracts obtained from *N.*  
248 *benthamiana* leaves transiently expressing the two proteins (Fig. 5).

249

250 We next performed co-localization experiments to determine the subcellular  
251 localization of the KAT1-BAG4 complex. We show that the signal corresponding to the  
252 KAT1-BAG4 complex co-localizes with an ER marker protein (ChFP-KDEL), thus lending  
253 support to the idea that BAG4 could be involved in KAT1 assembly at this organelle  
254 (Fig. 6). Pearson and Mander coefficient analyses indicate a strong degree of co-  
255 localization between the KAT1-BAG4 BiFC signal and the ER marker (0.75-0.97 and

256 0.88-0.99, respectively). By contrast, these same parameters for the KAT1-KAT1 BiFC  
257 interaction and the same ER marker indicated no co-localization, as expected (Pearson:  
258 -0.17-0.035 and Mander: 0.016-0.024). Since the signal for the complex is punctate and  
259 is not observed throughout the ER, we also performed co-localization experiments  
260 with the ER exit site (ERES) marker Sec24-mRFP and the transmembrane domain of the  
261 rat  $\alpha$ -2,6-sialyltransferase fused to the Cherry fluorescent protein as a Golgi marker  
262 (STtmd-ChFP). We observed co-localization of the KAT1-BAG4 complex with the ERES  
263 marker (Pearson: 0.43-0.82 and Mander: 0.5-0.98), but not the Golgi marker (Pearson:  
264 -0.0039-0.042 and Mander: 0.1-0.5).

265

266 Interestingly, KAT1 was previously shown to interact with Sec24 through its di-acidic  
267 ER export signal motif (Sieben et al., 2008). Thus, our data confirm the interaction  
268 between BAG4 and KAT1 in a plant model system and show that the KAT1-BAG4  
269 interaction likely takes place at ERES, possibly facilitating its incorporation in coat  
270 protein complex II (COPII) vesicles. This is not unexpected as KAT1, like essentially all  
271 multi-span plasma membrane proteins, before arriving to the cell surface transits  
272 through the ER, where the protein is thought to be assembled into tetramers to form a  
273 functional channel that will be inserted into the plasma membrane via the secretory  
274 pathway. Our data suggest that BAG4 interacts with KAT1 as it transits through this  
275 organelle on its way to the plasma membrane. This model is consistent with that  
276 proposed for mammalian BAG proteins that are involved in the regulation of  
277 potassium and chloride channels that also act at the ER in cooperation with Hsp70  
278 (Knapp et al., 2014; Hantouche et al., 2017).

279

280 Our results indicate that BAG4 favors KAT1 activity in yeast and oocytes and that the  
281 interaction appears to take place at the ER exit sites. We hypothesized that BAG4 acts  
282 to facilitate KAT1 transit out of the ER and thus would promote the arrival of active  
283 KAT1 channels at the plasma membrane. In order to test this model, we examined  
284 whether BAG4 influences the arrival of this channel to the plasma membrane. Our first  
285 approach was to observe the time course of KAT1 plasma membrane accumulation in  
286 the presence and absence of co-expression of BAG4 in *N. benthamiana*. As shown in  
287 Figure 7, when BAG4 is co-expressed, a higher percentage of KAT1 protein is present at

288 the plasma membrane on day 1 after infiltration, whereas in the absence of BAG4,  
289 KAT1 accumulation at the plasma membrane is not comparable to that observed for  
290 KAT1\_BAG4 until day 3. Figure 7 shows representative images on each day with  
291 sufficient signal to clearly visualize KAT1 distribution and the quantification of the  
292 percentage of the total KAT1-YFP signal present at the plasma membrane for each  
293 condition and time point (n =10 cells). This result is consistent with ectopic BAG4  
294 expression facilitating the assembly of KAT1 containing tetramers and/or their delivery  
295 to the plasma membrane, which would in turn favor the accumulation of active  
296 channels at the plasma membrane. Since both the yeast and oocyte experiments  
297 suggest that BAG4 does not affect overall KAT1 protein accumulation, we tested  
298 whether this was also the case in this plant model system. As described in materials  
299 and methods, for these transient expression experiments we constructed vectors  
300 containing multiple transcriptional units, including an internal control for infiltration  
301 efficiency (dsRED containing an HA tag) within the same plasmid. Plants were  
302 agroinfiltrated with strains containing KAT1-YFP:dsRED-HA alone or KAT1-YFP:dsRED-  
303 HA:BAG4-myc. We analyzed the amount of KAT1-YFP and the internal control (dsRED-  
304 HA) in the infiltrated areas using the same time course. As shown in Figure 7, BAG4 co-  
305 expression does not increase the steady state amount of KAT1 protein. So, taken  
306 together, the data presented in Figures 7 clearly suggest that expression of BAG4  
307 promotes KAT1-YFP arrival at the plasma membrane.

308

309 In order to corroborate these observations, we carried out the opposite approach. We  
310 investigated the localization of KAT1 in Col-0 wild type plants and in *bag4* mutant lines  
311 using transient expression in *A. thaliana* (Fig. 7). Employing the AGROBEST transient  
312 transformation protocol (Wu et al., 2014), we observed KAT1 accumulation at the  
313 plasma membrane in wild type control plants. However, under the same conditions, in  
314 *bag4* mutants, the KAT1 signal observed at the cell surface was markedly decreased  
315 and an accumulation of punctate staining was observed (Fig. 7). We could complement  
316 this defect of KAT1 plasma membrane targeting observed in the *bag4* mutant by  
317 employing vectors co-expressing BAG4 with KAT1. Figure 7 also shows the  
318 quantification of the percentage of the total KAT1 signal present at the plasma  
319 membrane for each condition tested (n = 10). We observed a much lower percentage

320 of KAT1-YFP at the plasma membrane in *bag4* mutants, as compared to the Col-0  
321 control. Moreover, KAT1-YFP plasma membrane localization is recovered when we  
322 functionally complement the *bag4* mutant. These results support the previous  
323 experiments and suggest that the presence of BAG4 promotes the arrival of KAT1 at  
324 the plasma membrane, possibly by facilitating its assembly and/or delivery to the cell  
325 surface possibly through their physical interaction at the ER exit sites.

326

327 In order to provide additional evidence showing that BAG4 is a physiologically relevant  
328 KAT1 regulator, we analyzed phenotypes related to KAT1 activity in Arabidopsis lines  
329 lacking or overexpressing the *BAG4* gene. Two independent *bag4* mutant lines and two  
330 Col-0 lines and one *kat1* line overexpressing *BAG4* were tested for stomatal opening  
331 dynamics. The *kat1* and *kat2* single mutants and the *kat1 kat2* double mutant were  
332 included for comparison. As shown in Figure 8, two mutant lines lacking the *BAG4* gene  
333 show a delay in stomatal opening under all conditions tested. We also observed an  
334 initial delay in stomatal opening in the *kat1* and *kat2* mutant lines in response to light  
335 treatment, but not potassium-containing opening buffer. Therefore, at high potassium  
336 concentrations, the simple mutants are able to open their stomata, likely due to the  
337 redundancy of inward rectifying potassium channels. This idea is supported by the  
338 phenotype observed for the *kat1 kat2* double mutant, which shows a marked delay in  
339 both light and opening buffer. On the other hand, we observed that the  
340 overexpression of *BAG4* in Col-0 leads to an increase in stomatal aperture and this  
341 response is attenuated in the *kat1* mutant overexpressing *BAG4* (Figure 8). The levels  
342 of expression of the BAG4 protein are shown in Supplemental Figure S2.

343

344 As a complementary approach, we measured the temperature of the different mutants  
345 and BAG4 gain and loss-of-function lines using infrared thermography (Figure 9).  
346 Several studies have shown that this technique can be used for analyzing mutants with  
347 altered stomatal function as a relationship exists between the temperature of the  
348 leaves and variations in stomatal conductance (Jones, 1999; Merlot et al., 2002; Wang  
349 et al., 2004). We observed the expected increase in temperature in the lines that  
350 showed delayed stomatal aperture dynamics and a decrease in temperature in the Col-  
351 0 lines overexpressing BAG4 (Figure 9). When these results are considered together,

352 they strongly suggest that BAG4 plays a physiologically relevant role in regulating  
353 potassium fluxes in stomata and possibly other cells. Importantly, the *BAG4* gene has  
354 been reported to be expressed in guard cells, which is a prerequisite for a  
355 physiologically relevant KAT1 regulator (Yang et al., 2008).

356

357 As discussed above, in the stomatal response assay, we observed additional  
358 phenotypes in the *bag4* mutant lines, as compared to the *kat1* or *kat2* simple mutants.  
359 These data suggest that BAG4 may regulate proteins in addition to KAT1, including  
360 other potassium channels, like KAT2. Lebaudy and collaborators showed the  
361 importance of the guard cell membrane inward K<sup>+</sup> channel (GCK<sub>in</sub>) activity in stomatal  
362 movement (Lebaudy et al., 2008), identifying KAT1 and KAT2 as the major  
363 contributors. Therefore, we studied whether BAG4 could interact with KAT2 in a BiFC  
364 assay in *N. benthamiana*. As shown in Figure 10, we observed a pattern of fluorescence  
365 very similar to that observed for the KAT1-BAG4 interaction, but observed no signal in  
366 the control combinations. We used the KAT2-KAT1 interaction as a positive control for  
367 these assays, showing a uniform interaction at the plasma membrane, similar to what  
368 we observed with the KAT1-KAT1 interaction (Figure 5), confirming the functionality of  
369 the KAT2 BiFC fusion. Although further studies are required to characterize the  
370 molecular details of these interactions and ascertain whether there are additional  
371 targets, our data suggest that BAG4 may act as a regulator of at least these two  
372 potassium channels and provide a plausible explanation for the results obtained in the  
373 stomatal response assays described.

374

## 375 **Discussion**

376 The regulation of ion fluxes in guard cells is crucial for stomatal movement, which is an  
377 important determinant of the plant's response to fluctuating environmental conditions  
378 (Lebaudy et al., 2008). Inward rectifying potassium channels are known to play  
379 important roles in this process. As such, these channels are predicted to be highly  
380 regulated and as expected, several proteins have been identified as regulators of the  
381 KAT1 channel (Sottocornola et al., 2006; Sottocornola et al., 2008; Sato et al., 2009;  
382 Eisenach et al., 2012; Ronzier et al., 2014; Zhang et al., 2015; Saponaro et al., 2017). In

383 this report, we describe the identification and initial characterization of a KAT1  
384 regulator that we recovered in a split-ubiquitin screening in yeast. The BAG4 protein  
385 was found to physically interact with KAT1 and also to increase potassium uptake in  
386 yeast. In oocytes, a similar phenomenon was observed, as increased KAT1 currents  
387 were observed one day after injection. Thus, our data clearly indicate that in two  
388 heterologous systems, BAG4 co-expression increases KAT1 transport activity, likely by  
389 increasing the number of active channels at the membrane. It is very unlikely that this  
390 regulation is at the transcriptional level in these model organisms, since we could show  
391 that the total amount of KAT1 does not change upon BAG4 co-expression in yeast and  
392 in the oocyte experiments, the same amount of KAT1 cRNA is injected in both cases.

393 We provide experimental evidence for the physical interaction between KAT1 and  
394 BAG4 in plants using two complementary approaches, BiFC and co-  
395 immunoprecipitation. The signal corresponding to the KAT1-BAG4 complex co-localizes  
396 with a general ER marker and with an ER exit site marker, which supports the notion  
397 that BAG4 could be involved in KAT1 assembly at this organelle. BAG4 is a member of a  
398 highly conserved family of proteins that all contain a characteristic BAG domain. This  
399 domain has been shown to interact with the Hsp70 chaperone in both mammals and  
400 plants (Takayama and Reed, 2001; Doukhanina et al., 2006; Kabbage and Dickman,  
401 2008; Lee et al., 2016). On the other hand, Hsp70 has been shown to be required for  
402 the assembly of the mammalian potassium channel, hERG1 at the ER (Li et al., 2017).  
403 Given the role for the BAG proteins documented in mammals and our observations in  
404 yeast and oocytes, we hypothesized that BAG4 may be implicated in the arrival of  
405 KAT1 to the plasma membrane, likely at the level of protein folding, tetramer assembly  
406 and/or trafficking. We provide experimental evidence supporting this idea using both  
407 gain- and loss-of-function experiments, where we observe an improvement in KAT1  
408 plasma membrane arrival upon BAG4 expression and a delay in its accumulation at the  
409 plasma membrane in lines lacking the *BAG4* gene. Importantly, we show that the total  
410 amount of KAT1 is not affected by BAG4 co-expression, but the percentage of KAT1  
411 that arrives at the plasma membrane is increased. Taken together, these data suggest  
412 that the modulation of a step required for KAT1 channel assembly, ER exit and/or  
413 plasma membrane delivery may be one of the functions of the BAG4 protein.

414 Several studies have addressed KAT1 trafficking and its regulation. For example,  
415 efficient transport of KAT1 to the plasma membrane is mediated by a di-acidic ER  
416 export signal in the C-terminus of the protein, which binds to the Sec24 component of  
417 coat protein complex II (COPII) (Hurst et al., 2004; Meckel et al., 2004; Sieben et al.,  
418 2008). Here, we observed the co-localization of the KAT1-BAG4 complex with Sec24,  
419 which has been described as a marker of ER exit sites (reviewed in (Matheson et al.,  
420 2006; Langhans et al., 2012)). Therefore, BAG4 may regulate this step of KAT1  
421 processing as it moves out of the ER through the secretory pathway towards the  
422 plasma membrane. It has also been shown that abscisic acid stimulates the  
423 endocytosis of KAT1 in both epidermal and guard cells, which can then recycle back to  
424 the plasma membrane when the levels of the hormone decrease (Sutter et al., 2007).  
425 In addition, two trafficking related proteins, SYP121 and VAMP721 are involved in  
426 regulating KAT1 delivery and recycling, and more recently have been shown to  
427 regulate channel gating (Sutter et al., 2006; Eisenach et al., 2012; Zhang et al., 2015;  
428 Zhang et al., 2017; Lefoulon et al., 2018). Whether BAG4 is related to any of these  
429 known regulatory mechanisms is an interesting question for future studies.

430 In plants, there are seven members of the BAG family and different phenotypes have  
431 been attributed to the *bag1*, *bag4* and *bag6* loss-of-function mutants, suggesting that  
432 each family member may carry out distinct functions (Doukhanina et al., 2006;  
433 Kabbage et al., 2016; Lee et al., 2016). Moreover, high throughput studies have  
434 indicated that, for example, both *BAG4* and *BAG1* are expressed in guard cells,  
435 whereas *BAG7* expression is low in this cell type (Winter et al., 2007). In order to study  
436 the specificity of the KAT1-BAG4 interaction, we used the split-ubiquitin and functional  
437 complementation assays to test whether two other BAG family members that share  
438 similar domain architecture, BAG1 and BAG7, interacted with KAT1. Our results show  
439 that the BAG protein with a higher level of conservation as compared to BAG4, BAG1  
440 showed a lower, but detectable level of interaction and regulation of KAT1 in yeast.  
441 However, a negligible level of interaction was observed for the more distantly related  
442 BAG7 protein, thus suggesting a considerable level of specificity for the KAT1-BAG4  
443 interaction.



444 In order to begin to establish BAG4 as a *bona fide* KAT1 regulator, we tested whether  
445 BAG4 may play a role in a physiological response in which this channel is implicated.  
446 Indeed, we observed a delay in stomatal aperture in two independent *bag4* mutant  
447 lines in response to external potassium and light. We observed a similar delay in  
448 stomatal aperture in response to light in the *kat1* and *kat2* mutant lines. Our data  
449 regarding the *kat1* mutant is in contrast to a previous report (Szyroki et al., 2001), but  
450 may be explained by differences in the time course studied and/or the mutant lines  
451 used. The line used here contains a T-DNA insertion in the first exon. In addition, we  
452 observed an increase in stomatal aperture in Col-0 lines overexpressing BAG4 and this  
453 response was reduced when the gene was overexpressed in a *kat1* mutant line. Thus,  
454 we were able to show that both loss- and gain-of-function of BAG4 affects stomatal  
455 aperture dynamics and that in the case of BAG4 overexpression, KAT1 is required to  
456 observe the full response.

457 We corroborated these results by measuring the temperature of the plants as an  
458 indirect measure of the transpiration rate. If the stomatal aperture is decreased in  
459 *bag4* mutants, so is the rate of transpiration and therefore, the temperature of the  
460 leaves of these plants would be expected to be higher. Our results show that lines  
461 lacking the BAG4 gene display an increased temperature, again adding support to its  
462 role in regulating ion fluxes important for stomatal movement. As expected, double  
463 mutants lacking both the KAT1 and KAT2 genes have a more pronounced phenotype.  
464 Moreover, Col-0 lines overexpressing BAG4 display lower leaf temperatures, which is  
465 in agreement with the data regarding stomatal aperture. Taken together, our results  
466 establish a role for BAG4 in the regulation of stomatal aperture dynamics through the  
467 regulation of the KAT1 inward rectifying potassium channel.

468 It is interesting to note that the two *bag4* mutant lines showed a longer delay in  
469 stomatal opening in response to opening buffer, which was not observed in the *kat1*  
470 and *kat2* single mutants but was observed in the *kat1 kat2* double mutant. BAG  
471 proteins are very likely to regulate many different proteins and in terms of stomatal  
472 aperture, other inward rectifying potassium channels, like KAT2, AKT1, and AKT2/3 are  
473 known to contribute to this response and our genetic data suggest a role for KAT2.  
474 Thus, we tested whether BAG4 could also interact with KAT2 in plants. Our results

475 using the BiFC assay show a KAT2-BAG4 interaction. Thus, it appears that BAG4  
476 regulates both KAT1 and KAT2, but we cannot rule out other channels as additional  
477 targets at this stage.

478 In mammalian systems, although BAG proteins have been related to many cellular  
479 processes, a specific role for BAG proteins in the regulation of ion channels has been  
480 reported. Both BAG1 and BAG2 have been shown to regulate the Cystic Fibrosis  
481 transmembrane conductance regulator (CFTR) chloride channel and BAG1 was more  
482 recently implicated in human Ether-à-go-go-related gene (hERG) potassium channel  
483 regulation (Young, 2014; Hantouche et al., 2017). In both cases, it appears that the  
484 BAG proteins mediate the misfolded protein response, thus likely playing a role in  
485 channel degradation, not plasma membrane delivery. Further experiments will be  
486 required to clarify the molecular mechanisms responsible for this apparent difference  
487 observed here for the plant BAG4 protein. The Arabidopsis BAG1 protein has been  
488 reported to be a co-factor in Hsc70-mediated proteasomal degradation of unimported  
489 plastid proteins, and so may have a function more analogous to its mammalian  
490 counterparts (Lee et al., 2016). However, our results identify BAG4 as a positive  
491 regulator of the KAT1 (and likely KAT2) potassium channel in plants and thus opens a  
492 novel line of investigation by linking the plant BAG family to the regulation of  
493 potassium channels and stomatal movement.

494

## 495 **Conclusions**

496 Taken together, the data presented here suggest that one main role for BAG4 in plants  
497 may be related to the post-translational regulation of ion channels and, consequently  
498 stomatal movement. Thus, BAG4 may constitute a novel target for the design of  
499 engineered crops with altered potassium fluxes, and concomitantly, improved water  
500 use efficiency and drought tolerance.

501

502

503

504

505

506

507

## 508 **Materials and Methods**

509 *Plant materials and plant growth.* The following Arabidopsis lines were employed: *kat1*  
510 mutant (SALK 093506, carrying the T-DNA insertion in the 1<sup>st</sup> exon), *kat2* mutant (SALK  
511 025933) and two *bag4* mutant lines SAIL\_144\_A10 (carrying the T-DNA insertion in the  
512 1<sup>st</sup> exon) and SALK\_033845 (carrying the T-DNA insertion in the 2<sup>nd</sup> exon) (obtained  
513 from the Salk Institute Genomic Analysis Laboratory and (Sessions et al., 2002).  
514 Arabidopsis plants were grown under an 8h light: 16h dark photoperiod at 22 °C in MS  
515 media supplemented with 1% sucrose. For stomatal movement and leaf temperature  
516 assays, after 2 weeks, plants were transplanted to soil and analyzed at 4-6 weeks.  
517 *Nicotiana benthamiana* plants were grown for 4-5 weeks in soil under an 16h light: 8h  
518 dark photoperiod at 24 °C.

519 *Yeast strains and plasmids.* The Split-ubiquitin KAT1 bait vector used for the screening  
520 was derived from the KAT1-pMetYCgate vector (ABRC CD3-815, (Obrdlik et al., 2004)).  
521 In order to carry out the screening, the AMP<sup>r</sup> marker was substituted with KAN<sup>r</sup> by  
522 recombination in yeast as follows: the kanamycin resistance gene was amplified with  
523 the primers Kan-F 5'-ttcttgaagacgaaagggcctcgtgatacgcctattTCCAGTTCGATTTATTC  
524 AACAAAG-3' and Kan-R 5'-taaagtatatatgagtaaacttggtctgacagttacGATCGATCCTAG  
525 TAAGCCACGTTG-3' and was co-transformed in the PLY240 strain (MATa *his3Δ200 leu2-*  
526 *3,112 trp1Δ901 ura3-52 suc2Δ9 trk1Δ51 trk2Δ50::lox-KanMX-lox*; (Bertl et al., 2003)  
527 together with the KAT1-pMETYCgate vector linearized with AatII. Clones growing in  
528 media lacking leucine were tested for growth in media containing 50 mM LiCl to select  
529 strains expressing KAT1. Plasmids were recovered from these yeast strains and  
530 transformed into DH5α and kanamycin resistant colonies were selected. The resulting  
531 plasmid was confirmed by sequencing. The cDNA library from 6-day-old *Arabidopsis*  
532 *thaliana* seedlings in the pDSL-Nx vector was obtained from Dualsystems Biotech AG.  
533 The screening was carried out in the THY.AP4 strain (MATa, *ura3, leu2, lexA::lacZ::trp1,*

534 *lexA::HIS3*, *lexA::ADE2*; (Paumi et al., 2007)). The BAG4 clone recovered in the  
535 screening lacks the sequence encoding the first 13 amino acids. The BAG1, BAG7 and  
536 full-length BAG4 plasmids were constructed by recombination into the pDSL-Nx vector  
537 in yeast using PCR products amplified from a cDNA library made from Arabidopsis  
538 seedlings.

539 *Split-ubiquitin screening.* The THY.AP4 strain containing the modified KAT1-Cub (KAT1-  
540 CubKAN<sup>r</sup>) plasmid was transformed with 20 micrograms of the *A. thaliana* cDNA library  
541 in the pDLSN-X vector (Dual Systems). Approximately  $8.6 \times 10^6$  transformants were  
542 analyzed for growth in selective media. The first 125 colonies growing in selective  
543 media were analyzed. Plasmids were recovered, re-transformed, tested for growth in  
544 selective media, classified by restriction analysis and subjected to specificity tests using  
545 the Ost3-Cub vector encoding a yeast oligosaccharyl transferase (Yan et al., 2005). The  
546 clones that passed these tests were then sequenced and analysed in the yeast  
547 functional complementation assay.

548 *Functional complementation assay in yeast.* The PLY240 strain was co-transformed  
549 with the KAT1-CubKAN<sup>r</sup> and the indicated pDLSN-X vectors and the empty vector  
550 corresponding controls. Pre-cultures were grown to saturation in SD media  
551 supplemented with auxotrophic requirements, 0.75 mg/mL methionine (to reduce  
552 KAT1 expression) and 0.1 M KCl. Fresh cultures (1:20 dilution) were grown for 16 hours  
553 in low potassium Translucent media supplemented with requirements and methionine  
554 (ForMedium™ UK; (Navarrete et al., 2010)) and diluted to OD<sub>600</sub> 0.2 in three different  
555 conditions of Translucent media supplemented with auxotrophic requirements: 1) low  
556 potassium, no methionine (low KCl, high KAT1 expression); low potassium, 0.75 mg/mL  
557 methionine (low KCl, low KAT1 expression) and 3) 0.1 M KCl, no methionine (high KCl,  
558 high *KAT1* expression). The Translucent media contains 12 μM K<sup>+</sup>. The optical density  
559 was determined periodically for 72 hours using a BioscreenC system (Oy Growth  
560 Curves Ab Ltd). Triplicate determinations were performed for at least 3 independent  
561 transformants for each plasmid combination. Similar results were observed in all  
562 experiments. Correct expression of each fusion protein was confirmed by immunoblot  
563 analysis of the corresponding whole cell extracts of cultures grown in Translucent  
564 media supplemented with 0.1 M KCl and 0.75 mg/mL methionine using anti-HA and

565 anti-LexA antibodies (Covance and Abcam, respectively), the corresponding anti-  
566 mouse or anti-rabbit HRP secondary antibodies and ECL detection system (GE  
567 Healthcare). Several independent clones were used for the quantification of KAT1  
568 protein expression in the absence and presence of BAG4. ImageJ was used to quantify  
569 the bands corresponding to the LexA signal and the loading control to calculate  
570 normalized KAT1 expression.

571 *Potassium consumption uptake and external acidification in yeast.* The indicated  
572 plasmids were transformed in the PLY240 background and grown as described above  
573 in the functional complementation assay to mid-log phase OD600 = 0.5-0.6 in  
574 Translucent media supplemented with auxotrophic requirements and 0.75 mg/mL  
575 methionine. Cells were collected by centrifugation, washed, resuspended in sterile  
576 water and incubated for 30 minutes at room temperature. External K<sup>+</sup> was monitored  
577 using external K<sup>+</sup>-selective mini-electrodes. Single-barrelled borosilicate glass  
578 capillaries, 7 cm long and of 1.5 mm of external diameter, were pulled in a patch clamp  
579 puller to get an open tip. Then, capillaries were silyanized and back-filled with K<sup>+</sup>  
580 ionophore I sensor (cocktail B, cat. No. 60398; Fluka, now part of Sigma) dissolved in a  
581 mixture of polyvinyl-chloride/tetrahydrofuran (40 mg/mL) at a ratio of 30:70 (v/v), as  
582 was previously described (Planes et al., 2015). For the assays, approximately 20 mg of  
583 cells (wet weight) were resuspended in 3 mL of 10 mM MES pH 4.0 and loaded in a  
584 temperature controlled (20 °C) plexiglass cylinder chamber under continuous stirring.  
585 K<sup>+</sup>-selective and reference electrode tips were placed in the assay medium and  
586 connected to a high-impedance differential amplifier (FD223; World Precision  
587 Instruments). In addition, a single glass pH electrode (model 5209, Crison) was also  
588 submerged into the assay medium in order to measure the external acidification to  
589 check the activation of the proton ATPase. After steady readings of both pH and  
590 external potassium K<sup>+</sup> signals were obtained, potassium chloride was added to a final  
591 concentration of 1 mM and then, after stable readings values were again attained, 20  
592 mM of glucose were added to activate the proton ATPase, Pma1 and energize  
593 potassium uptake. Both the external pH and the potassium concentration were  
594 recorded for 45 minutes after glucose addition. The K<sup>+</sup> electrode signal was calibrated  
595 before and after experiments by adding potassium chloride to final concentrations of

596 0.1, 0.5, 1 and 10 mM in the assay media. Calibration curves render slopes around 45  
597 mV per  $\text{pK}^+$  unit. Both the total uptake (after 45 minutes) and the initial rate of  $\text{K}^+$   
598 uptake (slope of the curve representing the initial uptake; 5-8 minutes) were  
599 determined for three independent clones of each plasmid combination indicated  
600 (Figures 3A and B, respectively).

601 *Two-electrode voltage clamp in Xenopus oocytes.* KAT1 and BAG4 coding regions were  
602 cloned into a modified pGEM-HE vector (D. Becker, University of Würzburg, Germany).  
603 cRNA were synthesized from 1  $\mu\text{g}$  of linearized vector using the HiScribe™ T7 ARCA  
604 mRNA (with tailing) kit (NEB, <http://www.NEB.com>). Oocytes were obtained and  
605 prepared as previously described (Véry et al., 1995) and were injected with 30 ng of  
606 KAT1 cRNA or co-injected with 30 ng of KAT1 cRNA and 22.5 ng of BAG4 cRNA using a  
607 pneumatic injector. One day after oocyte injection, currents from whole oocytes  
608 bathed in K100 medium (100 mM KCl, 2 mM  $\text{MgCl}_2$ , 1 mM  $\text{CaCl}_2$ , 10 mM HEPES/Tris pH  
609 6) were recorded using the two-electrode voltage clamp technique. Data acquisition  
610 and analyses were performed as previously described (Corratgé-Faillie et al., 2017).  
611 Voltage drops resulting from the series resistance of the bath were corrected by using  
612 two external electrodes connected to a bath probe (VG-2A x100 Virtual-ground bath  
613 clamp; Axon Instruments). KAT1 currents were obtained by subtraction of mean  
614 currents recorded in water-injected oocytes from the same oocyte batch. The  
615 percentage of KAT1 current increase with BAG4 = Mean current in the presence of  
616 BAG4 - Mean current in its absence / Mean current in its absence.

617 *BiFC and co-immunoprecipitation assays in Nicotiana benthamiana.* All KAT1 and BAG4  
618 plasmids used for the BiFC and co-immunoprecipitation experiments and to generate  
619 overexpression lines were constructed using the GoldenBraid system (Sarrion-  
620 Perdigones et al., 2013). For BiFC assays, we used pUPD2 vectors containing the YFN or  
621 YFC sequences from the GoldenBraid collection. Then, we cloned KAT1 and BAG4  
622 versions, compatible with the cloning system into the pUPD2 vector. Alpha vectors  
623 containing the indicated fusion proteins and the 35S promoter and Tnos terminator  
624 were assembled and combined to generate the omega level plasmids that were  
625 transformed into the *Agrobacterium tumifaciens* strain C58Ci. For indicated  
626 experiments, alpha level plasmids were constructed from these omega plasmids to

627 generate constructs containing 3 or 4 transcriptional units. For plant infiltration, we  
628 used 4- to 5-week-old *N. benthamiana* plants grown at 24 °C under a 16h light: 8h dark  
629 photoperiod. For co-localization experiments used to determine the subcellular  
630 localization of the complex, the *KAT1-BAG4* interacting combination was co-infiltrated  
631 with a second plasmid containing either the ER marker (calreticulin targeting  
632 sequence-Cherry fluorescent protein-KDEL retention sequence (ChFP-KDEL)), the  
633 Sec24-RFP ER exit site (ERES) marker (both kindly provided by V. Pallás, IBMCP, Spain),  
634 or the transmembrane domain of the rat  $\alpha$ -2,6-sialyltransferase enzyme fused to the  
635 Cherry fluorescent protein as a Golgi marker (STtmd-ChFP) (Prokhnevsky et al., 2005).  
636 An agrobacterium strain (C58Ci) transformed with the plasmid encoding the P19  
637 Tomato Bushy Stunt Virus silencing suppressor was also used in all the infiltrations  
638 (Sarrion-Perdigones et al., 2013). The images were acquired using a Zeiss fluorescence  
639 confocal microscope with the following settings: YFP was excited with an Argon laser  
640 (514 nm) and detected at 516-548 nm. Cherry, RFP and dsRED fluorescent proteins  
641 were excited using the DPSS 561-10 laser (561 nm) and detected at 580-650 nm.  
642 Chloroplast autofluorescence was detected between 675 and 760 nm. The statistical  
643 analyses for *KAT1-BAG4* BiFC and the organelle makers were determined by calculating  
644 the Pearson and Mander coefficients (corresponding to the range of values obtained in  
645 4 independent images) (Dunn et al., 2011). For co-IP assays, we used a pUPD2 4x-c-myc  
646 sequence from the Addgene collection, to create the c-myc-BAG4 fusion. We  
647 combined the *KAT1-YFP* and c-myc-BAG4 alpha vectors to build the omega plasmid  
648 containing both fusion proteins and infiltrated *N. benthamiana* leaves. Extraction of  
649 total proteins was carried out in modified PBS buffer (140 mM NaCl, 8 mM  
650 Na<sub>2</sub>HPO<sub>4</sub>·7H<sub>2</sub>O, 2 mM KH<sub>2</sub>PO<sub>4</sub>, 10 mM KCl, Proteinase Inhibitor, pH 7.4). The *KAT1-YFP*  
651 protein was purified using the GFP-trap (GFP-Trap<sup>®</sup>\_MA, Chromotech) according to the  
652 manufacturer's instructions. Samples of the protein extracts, the unbound material  
653 and the *KAT1* purification were separated on 8% SDS-PAGE gels, transferred to  
654 nitrocellulose membranes and probed with an anti-GFP antibody (clone 7.1 and 13.1  
655 mixture, Roche) and an anti-c-myc antibody (clone 9E10, Roche) to detect BAG4.  
656 Immune complexes were visualized using the corresponding anti-mouse or anti-rabbit  
657 HRP secondary antibodies and ECL detection system (GE Healthcare).  
658

659 *Kinetics of plasma membrane accumulation in N. benthamiana and A. thaliana*

660 For transient expression in *N. benthamiana*, leaves were infiltrated, treated and  
661 imaged as described for BiFC and Co-IP. However, in this case P19 silencing suppressor  
662 was not added to the infection mixture. The ImageJ program was used to quantify the  
663 percentage of KAT1-YFP present at the plasma membrane as follows: the free draw  
664 tool was used to trace the contour of individual cells, directly adjacent to the cell  
665 boarder (inside cell fluorescence). These forms were digitally enlarged by 7 pixel units  
666 using the ImageJ tool to quantify the whole cell fluorescence. Fluorescence levels in  
667 ellipses adjacent to the cells were also quantified and used as the background  
668 measurement. The corrected total cell fluorescence (CTCF) was calculated using the  
669 following formula: Integrated Density – (area of selected cell × mean fluorescence of  
670 background readings). The percentage of fluorescence signal at the plasma membrane  
671 was then calculated using the following formula: % fluorescence PM = 100 –  
672  $\left( \frac{\text{CTF inside fluorescence}}{\text{CTF whole cell fluorescence}} * 100 \right)$ . This procedure was carried out for 10 individual cells  
673 from each of the indicated conditions deriving from experiments done on different  
674 days. In order to quantify the amount of KAT1 protein with and without BAG4 co-  
675 expression, an alpha1 level plasmid was constructed to combine the KAT1-YFP\_myc-  
676 BAG4 omega construct (or the control) with the dsRED protein which incorporates an  
677 HA epitope tag (dsRED-HA) in the same vector. In this way, the amount of dsRED can  
678 be used as an internal control monitoring the level of transient expression in each case  
679 because all transcriptional units are in the same plasmid. Infected plants were  
680 observed on days 1, 2 and 3 post-infiltration by fluorescence confocal microscopy and  
681 whole cell protein extracts were generated from the infiltrated material by grinding 2  
682 cm leaf discs in SDS-PAGE loading buffer. Samples were separated on SDS-PAGE,  
683 transferred and KAT1, BAG4 and dsRED were detected using anti-GFP, anti-c-myc and  
684 anti-HA antibodies.

685 For transient expression in Arabidopsis, the Col-0 control and the *bag4* mutant lines  
686 (SALK\_033845 and SAIL\_144\_A10) were agroinfiltrated following the AGROBEST  
687 protocol (Wu et al., 2014). The plasmid used was the alpha level plasmid containing  
688 KAT1-VENUS<sub>intron</sub> which included an intron in the Venus sequence (kindly provided by  
689 Stan Gelvin, Purdue University, USA). This was required to avoid expression of the



690 KAT1 fusion protein in the agrobacterium strain. An omega vector combining the KAT1-  
691 VENUS<sub>intron</sub> and myc-BAG4 transcriptional units was used for the complementation  
692 assays. Confocal images were acquired as described above using the 514 laser and an  
693 emission wavelength between 515 nm and 530 nm. The quantification of the amount  
694 of KAT1-YFP at the plasma membrane was calculated as described above for 10  
695 individual cells from each condition indicated.

696

697 *Stomatal movement assays.* The following lines were employed: *kat1* mutant (SALK  
698 093506, carrying the T-DNA insertion in the 1<sup>st</sup> exon), *kat2* mutant (SALK 025933) and  
699 the two *bag4* mutant lines SAIL\_144\_A10 (carrying the T-DNA insertion in the 1<sup>st</sup> exon)  
700 and SALK\_033845 (carrying the T-DNA insertion in the 2<sup>nd</sup> exon) (obtained from the  
701 Salk Institute Genomic Analysis Laboratory and (Sessions et al., 2002), two  
702 independent transformants that are homozygous for the *BAG4* insertion in the Col-0  
703 and *kat1* mutant (SALK 093506, carrying the T-DNA insertion in the 1<sup>st</sup> exon) lines  
704 generated by the floral dipping method using an omega level plasmid containing the c-  
705 myc-BAG4 fusion and the BASTA resistance gene. The double *kat1 kat2* mutant was  
706 generated by crossing the single mutants listed above. Plants were grown 4-6 weeks  
707 under an 8h light: 16h dark photoperiod at 22 °C. Five leaves (each taken from  
708 different plants) from each genotype and condition were analysed. For the dark  
709 conditions, leaves were harvested 1 hour before the lights switched on and the leaf  
710 was split into two halves: one was maintained in the dark in MES solution, while the  
711 other was incubated in stomatal opening buffer (10 mM KCl, 7.5 mM iminodiacetic  
712 acid; 10 mM MES/Tris pH 6.2), for 2.5 hours. For light treatment, the leaf was split into  
713 two halves and both were kept in 10 mM MES (pH 5.6). One half was kept in the dark  
714 and the other exposed to light and observed 2.5 hours later. To take stomatal images,  
715 the tissue was mounted on a microscope slide and immersed in the respective  
716 solution. The stomatal aperture was defined as the ratio between the length of the  
717 stomatal aperture from the point of junction of the inner lips and the maximal width  
718 between the inner cuticular lips. For each condition, between 60 and 100 stomata  
719 were analyzed in five different plants. The entire assay was repeated three times.

720

721 *Leaf temperature measurements.* The same lines used in the stomatal movement  
722 assays were grown under an 8h light: 16h dark photoperiod at 22 °C. The  
723 thermographic camera Bosch GTC 400 C was used to generate the infrared images of  
724 the plants 1.5 hours after the lights turned on. The plants were sown in individual pots  
725 such that the rosette leaves were not touching the walls of the pot, the tray or other  
726 plants. For imaging, each plant was moved to a tray partially filled with water, to  
727 create a uniform environmental temperature around the pot. Leaf temperature was  
728 calculated using the GTC Transfer Software. A total of 6 plants were measured for each  
729 genotype. Ten points were measured for each plant (60 data points/genotype). Data  
730 from each genotype were pooled together and statistically analyzed (Student *t*-test)  
731 using the Graph Prism6 software.

732

### 733 **Accession Numbers**

734 Sequence data from this article can be found in the GenBank data libraries under  
735 accession numbers: *AtKAT1*, At5g46240; *AtKAT2*, At4g18290; *AtBAG4*, At3g51780.  
736 Mutants used in this article can be obtained from the Arabidopsis Biological Resource  
737 Center under the following accession numbers: *kat1* mutant (SALK 093506), *kat2*  
738 mutant (SALK 025933), and *bag4* mutant lines (SAIL\_144\_A10) and (SALK\_033845).

739

### 740 **Supplemental Data**

741 Supplemental Figure S1. BAG4 co-expression favors early activity of KAT1 in *Xenopus*  
742 oocytes.

743 Supplemental Figure S2. Immunodetection of myc-BAG4 protein in homozygous  
744 transgenic lines.

745

### 746 **Acknowledgements**

747 The authors would like to thank Elena Moreno, María José Falaguer, Alejandro Mossi,  
748 Sara Aljama, José Antonio Navarro, Vicente Pallás, Daniel Franco-Aragón, Jorge Lozano,  
749 and Stan Gelvin for assistance in the completion of this work and for providing  
750 reagents.

751



753 **Figure Legends**

754 **Figure 1. Effect of the co-expression of interacting proteins on the functional**  
755 **complementation by KAT1 in yeast.** A) The indicated plasmids were co-transformed in  
756 the *trk1 trk2* mutant strain (PLY240) and the growth of the strains was assayed as  
757 described in Materials and Methods using the Translucent media (which contains 12  
758  $\mu\text{M}$  potassium) with or without methionine supplementation to decrease the  
759 expression of KAT1 (under control of the *MET25* promoter). The graph shows the  
760 average value of the optical density at 72 hours for triplicate determinations and the  
761 experiment was done with at least 3 independent transformants for each plasmid  
762 combination. (Translucent media with no KCl supplementation = Low KCl (12  $\mu\text{M}$   $\text{K}^+$ );  
763 Translucent media containing 0.75 mg/mL methionine = Low KAT1; Translucent media  
764 + 50 mM KCl added = High KCl; Translucent media +/- KCl without methionine = High  
765 KAT1). Data presented are the mean  $\pm$ SD and similar results were observed for three  
766 independent transformants. Asterisks (\*\*) indicate statistical significance (Student *t*-  
767 test) with a *p* value < 0.01. B) Immunoblot analysis of protein extracts from the  
768 indicated strains showing the correct expression of each of the fusion proteins. The  
769 KAT1 bait vector protein is detected with the anti-LexA antibody and the prey proteins  
770 with the anti-HA antibody. Results for a representative clone are shown. The long  
771 exposure is included to visualize the expression of the RPT2 prey protein, which  
772 accumulates less than the other two prey proteins. C) The KAT1 signal and the  
773 corresponding loading control were quantified using the ImageJ software and the  
774 average values of KAT1/loading control (Normalized KAT1) was calculated for 6 control  
775 strains (KAT1\_empty vector) and 7 KAT1\_BAG4 strains. Data presented are the mean  
776  $\pm$ SD.

777

778 **Figure 2. Study of the specificity of the interaction between KAT1 and other BAG**  
779 **family members.** A) The indicated plasmids were transformed into the THY.AP4 strain  
780 and grown to saturation in selective media. Serial dilutions were spotted onto media  
781 with the indicated composition to test for the protein-protein interaction between  
782 KAT1 and the indicated BAG family proteins. Identical results were observed for four  
783 independent clones. B) Immunoblot analysis of protein extracts from the indicated

784 strains showing the correct expression of each of the fusion proteins. The KAT1 bait  
785 protein is detected with the anti-LexA antibody and the prey proteins with the anti-HA  
786 antibody. Results for a representative clone are shown. C) The indicated plasmids were  
787 co-transformed in the *trk1 trk2* mutant strain (PLY240) and the growth of the strains  
788 was assayed as described in Figure 1A. The average value of triplicate determinations  
789 of the optical density of the growth normalized to the potassium-supplemented media  
790 is shown for each strain. Data presented are the mean  $\pm$ SD and similar results were  
791 observed for 3 independent clones of each plasmid combination. Asterisks (\*\*\*)  
792 indicate statistical significance (Student *t*-test) with a *p* value < 0.001 compared to the  
793 KAT1\_∅ control strain.

794

795 **Figure 3. Potassium uptake and external acidification.** The indicated plasmids were  
796 co-transformed in the *trk1 trk2* mutant strain (PLY240) and the strains were grown in  
797 low KCl and low KAT1 conditions and processed as described in Materials and  
798 Methods. A) The bars represent the average value for three independent experiments  
799 for the total potassium uptake for 45 minutes expressed as  $\mu\text{mol K}^+/\text{mg cells} \pm\text{SD}$ . B)  
800 The bars represent the average value for three independent experiments for the initial  
801 rate of potassium uptake expressed as  $\mu\text{mol K}^+/\text{min} \cdot \text{mg cells}$  calculated using the  
802 slope of the depletion curve (first 5-18 minutes) normalized to the wet weight of the  
803 cells  $\pm\text{SD}$ . C) The bars represent the average value for three independent experiments  
804 of the change in the pH value measured in parallel with the potassium consumption  
805  $\pm\text{SD}$ . The change in the external pH was determined during the first 15 minutes after  
806 glucose addition and was normalized to the wet weight of the cells. Asterisks (\*)  
807 indicate statistical significance (Student *t*-test) with a *p* value < 0.05.

808 **Figure 4. BAG4 co-expression increases KAT1 current in *Xenopus* oocytes.** A) Voltage-  
809 clamp protocol and representative current traces recorded by two-electrode voltage  
810 clamp in the presence of 100 mM KCl on oocytes co-expressing KAT1 or KAT1 and  
811 BAG4. B) KAT1 current (I) –voltage (V) relationships of oocytes co-expressing KAT1 and  
812 BAG4 (white circles) or expressing KAT1 alone (black circles). Data are means  $\pm$  SE (n=7  
813 for KAT1, n=11 for KAT1 + BAG4), and are representative of three experiments  
814 performed on different oocyte batches. C) Increase of mean KAT1 current upon BAG4

815 co-expression, at -110 mV (black) and at -155 mV (grey). Mean currents are from B). D)  
816 Voltage-dependence of KAT1-current activation in the presence of BAG4 (white circles)  
817 or with KAT1 expressed alone (black circles). Gating parameters ( $z$ , gating charge, and  
818  $E_{a50}$ , half-activation potential) were estimated by performing fits to the KAT1 I-V  
819 relationships (in the presence or absence of BAG4) with a Boltzmann function coupled  
820 to a linear relation (Lebaudy et al., 2010).  $G$ , KAT1 macroscopic conductance ( $G = I/V$ );  
821  $G_{max}$ , KAT1 macroscopic conductance at infinitely negative voltage.

822 **Figure 5. Confirmation of the interaction between KAT1 and BAG4 in *N.***  
823 ***benthamiana*.** Agrobacterium strains harbouring the indicated plasmids were used to  
824 infiltrate *N. benthamiana* leaves and images were obtained using fluorescence  
825 confocal microscopy 72 hours post-infiltration. A) Representative BiFC images for the  
826 KAT1-KAT1 interaction and control plasmids. The overlay of the grey scale and BiFC  
827 fluorescence is shown. Leaf epithelial cells and stomata are visible. B) Representative  
828 BiFC images for the KAT1-BAG4 interaction. Representative images of the experiments  
829 performed with the control plasmids are shown below. The red signal corresponds to  
830 chloroplast autofluorescence. For panels A and B, similar results were observed in at  
831 least four independent experiments performed on different days. (Bar = 20 $\mu$ m) C)  
832 Agrobacterium strains expressing the indicated plasmids were used to infiltrate *N.*  
833 *benthamiana* leaves. Samples were taken at 72 hours post-infiltration and processed  
834 for protein extraction and co-immunoprecipitation as described in Materials and  
835 Methods. The figure shows the results of the immunodetection using antibodies that  
836 recognize the BAG4 and KAT1 proteins. The amount of BAG4 recovered in the KAT1  
837 purification is shown in the first lane on the left. Similar results were observed in two  
838 independent experiments performed on different days. (YFN = N-terminal part of YFP;  
839 YFC=C-terminal part of YFP; IP=immunoprecipitation; FT=flow through).

840

841 **Figure 6. The KAT1-BAG4 complex co-localizes with the ER and ERES markers.** A) A  
842 plasmid containing the KAT1-BAG4 BiFC interaction and the ER marker ChFP-KDEL  
843 were infiltrated as described. The BiFC signal (right), ChFP signal (center), and the  
844 overlay image of the grey scale, BiFC fluorescence and the ChFP signals (left) are  
845 shown. Leaf epithelial cells and stomata are visible. B and C) The same co-localization

846 analysis of the KAT1-BAG4 complex was performed with the ER exit site marker, Sec24  
847 fused to RFP (Sec24-RFP) (B) and the STtmd-ChFP Golgi marker (C). The yellow arrows  
848 indicate the points of co-localization with the ER marker. Chloroplast autofluorescence  
849 is shown in blue. (Bar = 20 $\mu$ m). (YFN = N-terminal part of YFP; YFC=C-terminal part of  
850 YFP; ChFP=Cherry Fluorescent Protein; RFP=Red Fluorescent Protein; STtmd-ChFP= rat  
851  $\alpha$ -2,6-sialyltransferase transmembrane domain fused to the Cherry fluorescent  
852 protein).

853

854 **Figure 7. BAG4 expression effects the subcellular localization of KAT1.** A) Plasmids  
855 containing KAT1-YFP or both KAT1-YFP and BAG4 were transiently expressed in *N.*  
856 *benthamiana* using agro-infiltration. The fluorescence signal was analysed by confocal  
857 microscopy 1-, 2- and 3-days post-infiltration. Representative images are shown. Leaf  
858 epithelial cells and stomata are visible. Similar results were observed in three  
859 independent experiments performed on different days. (Bar = 20 $\mu$ m) B) The  
860 percentage of the fluorescence signal present in the plasma membrane (PM) was  
861 quantified using ImageJ, as described in Materials and Methods. The graph shows the  
862 average values  $\pm$ SD for 10 cells for each condition tested. C) Similar experiments as  
863 described in panel A were performed, but using GoldenBraid plasmids containing  
864 KAT1-YFP:dsRED-HA or KAT1-YFP:myc-BAG4:dsRED-HA. Whole cell extracts were  
865 prepared from infiltrated areas (previously confirmed to express KAT1-YFP) and  
866 proteins were processed for immunodetection. The dsRED-HA protein serves as an  
867 internal control for the efficiency of transient expression. (DAY PI= Day post-  
868 infiltration). D) The KAT1-VENUS<sub>intron</sub> (KAT1-VENUS<sub>i</sub>, top row) or the KAT1-  
869 VENUS<sub>intron</sub>\_BAG4 (bottom row) plasmids were transiently expressed in the Col-0 and  
870 the *bag4* mutant Arabidopsis lines using agro-infiltration. The fluorescence signal was  
871 analyzed by confocal microscopy 2 days after infiltration. Representative images are  
872 shown and similar results were observed in three independent experiments. Leaf  
873 epithelial cells and stomata are visible. (Bar = 20 $\mu$ m). E) The percentage of the  
874 fluorescence signal present in the plasma membrane (PM) was quantified using  
875 ImageJ, as described in Materials and Methods. The graph shows the average values  
876  $\pm$ SD for 10 cells for each condition tested. (Student *t*-test) (\*\*: p value <0.01).

877

878 **Figure 8. Effect of BAG4 loss and gain-of-function on stomatal aperture.** Stomata  
879 from the indicated Arabidopsis lines were analyzed as described in Materials and  
880 Methods. The data show the average ratio for 60-100 stomata  $\pm$ SD. A) The  
881 width/length ratio of stomata of the different mutant lines were determined in leaves  
882 from the indicated lines harvested 1 hour before the lights turned on (Dark), incubated  
883 for 2.5 hours in opening buffer in the dark (Opening buffer, O.B.) or 2.5 hours after the  
884 lights turned on (Light). Similar results were observed in three independent  
885 experiments. B) The width/length ratio of stomata of control lines and Col-0 and *kat1*  
886 homozygous for 35S:*BAG4* transgene were determined as described in panel A. For  
887 both experiments, the asterisks indicate statistical significance as compared to the Col-  
888 0 dark control (Student *t*-test) (\*\*: p value <0.01; \*\*\*: p value < 0.001; \*\*\*\* p value <  
889 0.0001). The length/width ratio was also significantly increased in *BAG4*  
890 overexpressing lines in both light and opening buffer (# indicates statistical comparison  
891 with Col-0 O.B. and ■ indicates statistical comparison with Col-0 light).

892

893 **Figure 9. Effect of BAG4 loss and gain-of-function on leaf temperature.** The same lines  
894 described in Figure 8 were analyzed for leaf temperature using an infrared  
895 thermography, as described in Materials and Methods (Panel A mutant lines, Panel B  
896 35S:*BAG4* lines). Each symbol represents an individual measurement and the bar  
897 represents the average value for 10 measurements of 6 different plants for each  
898 genotype. The error bars represent the standard deviation. For both experiments, the  
899 asterisks indicate statistical significance as compared to the Col-0 control or the  
900 comparisons indicated by the brackets above the graphs (Student *t*-test) (\*\*: p value  
901 <0.01; \*\*\*: p value < 0.001; \*\*\*\* p value < 0.0001).

902

903 **Figure 10. BAG4 interacts with KAT2 in BiFC assays in *N. benthamiana*.** Interaction  
904 assays were carried out and analyzed as described in the legend to Figure 5. Leaf  
905 epithelial cells and stomata are visible. As shown, a similar pattern of interaction is  
906 observed for KAT2 when tested with BAG4 (compare with Figure 5B). The BiFC signals  
907 corresponding to the KAT2-KAT1 and KAT2-BAG4 interactions are shown in green and  
908 the chloroplast autofluorescence is shown in red. (YFN = N-terminal part of YFP;  
909 YFC=C-terminal part of YFP). (Bar = 20 $\mu$ m).



910

911

912 **Literature Cited**

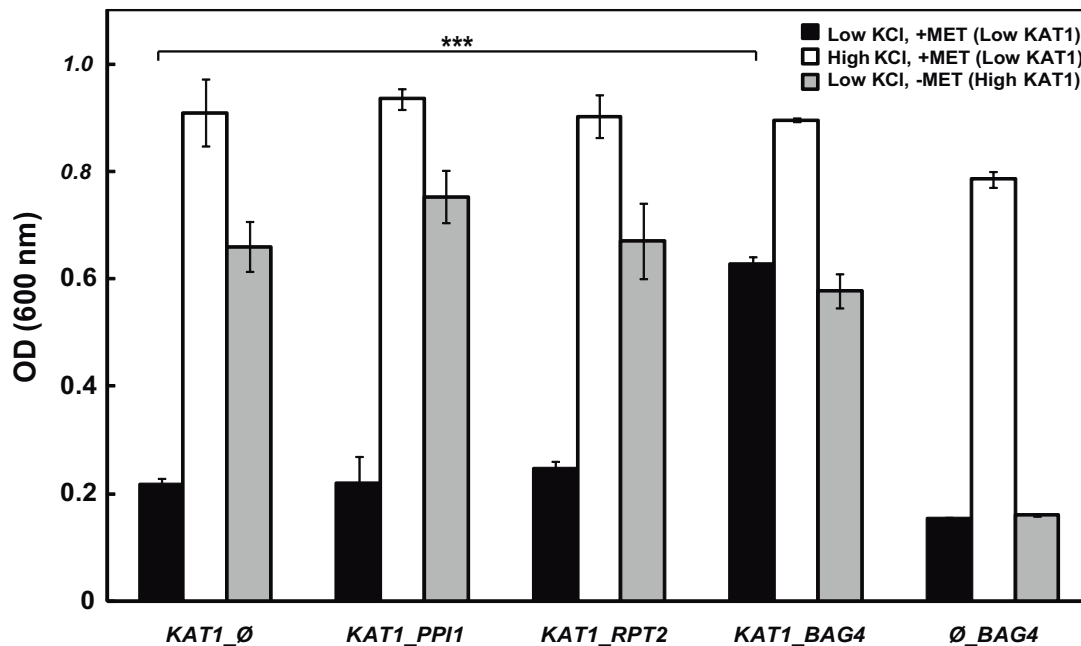
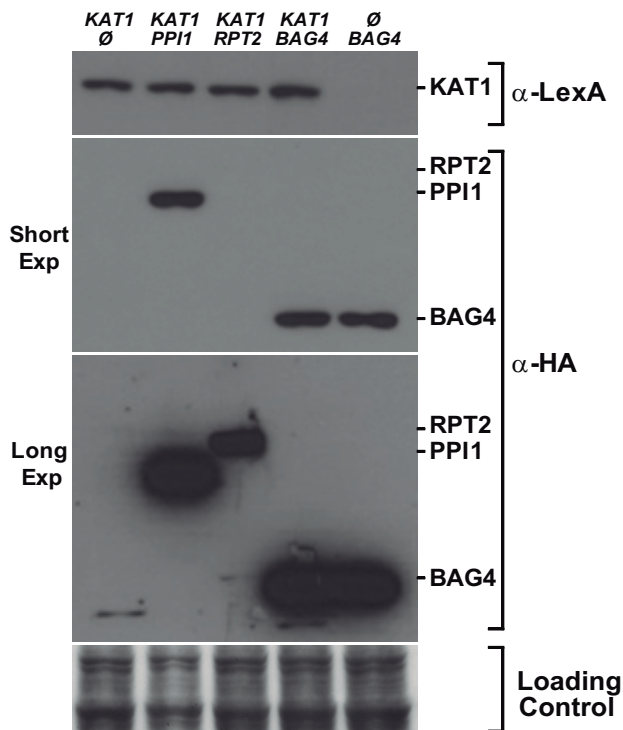
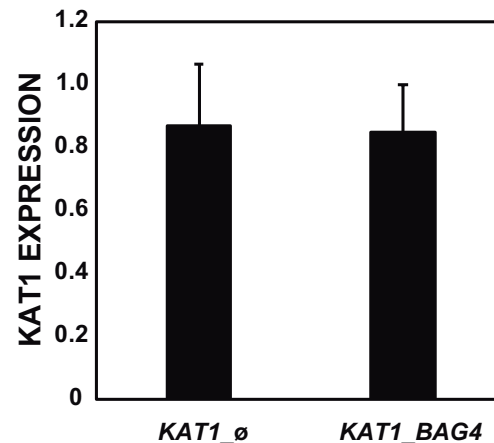
- 913 **Anderson JA, Huprikar SS, Kochian L V, Lucas WJ, Gaber RF** (1992) Functional expression of a  
914 probable *Arabidopsis thaliana* potassium channel in *Saccharomyces cerevisiae*. *Proc Natl*  
915 *Acad Sci U S A* **89**: 3736–3740
- 916 **Bertl A, Ramos J, Ludwig J, Lichtenberg-Fraté H, Reid J, Bihler H, Calero F, Martínez P,**  
917 **Ljungdahl PO** (2003) Characterization of potassium transport in wild-type and isogenic  
918 yeast strains carrying all combinations of *trk1*, *trk2* and *tok1* null mutations. **47**: 767–780
- 919 **Doukhanina E V., Chen S, Van Der Zalm E, Godzik A, Reed J, Dickman MB** (2006) Identification  
920 and functional characterization of the BAG protein family in *Arabidopsis thaliana*. *J Biol*  
921 *Chem.* doi: 10.1074/jbc.M511794200
- 922 **Dreyer I, Antunes S, Hoshi T, Müller-Röber B, Palme K, Pongs O, Reintanz B, Hedrich R** (1997)  
923 Plant K<sup>+</sup> channel alpha-subunits assemble indiscriminately. *Biophys J* **72**: 2143–2150
- 924 **Duby G, Hosy E, Fizames C, Alcon C, Costa A, Sentenac H, Thibaud JB** (2008) AtKC1, a  
925 conditionally targeted Shaker-type subunit, regulates the activity of plant K<sup>+</sup> channels.  
926 *Plant J* **53**: 115–123
- 927 **Dunn KW, Kamocka MM, McDonald JH** (2011) A practical guide to evaluating colocalization in  
928 biological microscopy. *Am J Physiol Cell Physiol* **300**: C723–42
- 929 **Eisenach C, Chen ZH, Grefen C, Blatt MR** (2012) The trafficking protein SYP121 of *Arabidopsis*  
930 connects programmed stomatal closure and K<sup>+</sup> channel activity with vegetative growth.  
931 *Plant J* **69**: 241–251
- 932 **Gierth M, Mäser P** (2007) Potassium transporters in plants – Involvement in K<sup>+</sup> acquisition,  
933 redistribution and homeostasis. **581**: 2348–2356
- 934 **Grefen C, Chen Z, Honsbein A, Donald N, Hills A, Blatt MR** (2010) A novel motif essential for  
935 SNARE interaction with the K(+) channel KC1 and channel gating in *Arabidopsis*. *Plant Cell*  
936 **22**: 3076–3092
- 937 **Hantouche C, Williamson B, Valinsky WC, Solomon J, Shrier A, Young JC** (2017) Bag1 Co-  
938 chaperone Promotes TRC8 E3 Ligase-dependent Degradation of Misfolded Human Ether a  
939 Go-Go-related Gene (hERG) Potassium Channels. *J Biol Chem* **292**: 2287–2300
- 940 **Hoang TM, Moghaddam L, Williams B, Khanna H, Dale J, Mundree SG** (2015) Development of  
941 salinity tolerance in rice by constitutive-overexpression of genes involved in the  
942 regulation of programmed cell death. *Front Plant Sci* **6**: 175
- 943 **Honsbein A, Blatt MR, Grefen C** (2011) A molecular framework for coupling cellular volume  
944 and osmotic solute transport control. *J Exp Bot* **62**: 2363–2370
- 945 **Hurst AC, Meckel T, Tayefeh S, Thiel G, Homann U** (2004) Trafficking of the plant potassium  
946 inward rectifier KAT1 in guard cell protoplasts of *Vicia faba*. *Plant J* **37**: 391–397
- 947 **Ivashikina N, Becker D, Ache P, Meyerhoff O, Felle HH, Hedrich R** (2001) K(+) channel profile  
948 and electrical properties of *Arabidopsis* root hairs. *FEBS Lett* **508**: 463–469
- 949 **Jeanguenin L, Alcon C, Duby G, Boeglin M, Chérel I, Gaillard I, Zimmermann S, Sentenac H,**  
950 **Véry AA** (2011) AtKC1 is a general modulator of *Arabidopsis* inward Shaker channel  
951 activity. *Plant J* **67**: 570–582

- 952 **Jiang Y, Lee A, Chen J, Ruta V, Cadene M, Chait BT, MacKinnon R** (2003) X-ray structure of a  
953 voltage-dependent K<sup>+</sup> channel. *Nature* **423**: 33–41
- 954 **Jones HG** (1999) Use of thermography for quantitative studies of spatial and temporal  
955 variation of stomatal conductance over leaf surfaces. *Plant, Cell Environ* **22**: 1043–1055
- 956 **Kabbage M, Dickman MB** (2008) The BAG proteins: A ubiquitous family of chaperone  
957 regulators. *Cell Mol Life Sci* **65**: 1390–1402
- 958 **Kabbage M, Kessens R, Dickman MB** (2016) A plant Bcl-2-associated athanogene is  
959 proteolytically activated to confer fungal resistance. *Microb Cell* **3**: 224–226
- 960 **Knapp RT, Wong MJH, Kollmannsberger LK, Gassen NC, Kretzschmar A, Zschocke J, Hafner K,  
961 Young JC, Rein T** (2014) Hsp70 cochaperones HspBP1 and BAG-1M differentially regulate  
962 steroid hormone receptor function. *PLoS One* **9**: doi:10.1371/journal.pone.0085415
- 963 **Langhans M, Meckel T, Kress A, Lerich A, Robinson DG** (2012) ERES (ER exit sites) and the  
964 “Secretory Unit Concept.” *J Microsc* **247**: 48–59
- 965 **Lawson T, Blatt MR** (2014) Stomatal size, speed, and responsiveness impact on photosynthesis  
966 and water use efficiency. *Plant Physiol* **164**: 1556–1570
- 967 **Lebaudy A, Pascaud F, Véry AA, Alcon C, Dreyer I, Thibaud JB, Lacombe B** (2010) Preferential  
968 KAT1-KAT2 heteromerization determines inward K<sup>+</sup> current properties in Arabidopsis  
969 guard cells. *J Biol Chem* **285**: 6265–6274
- 970 **Lebaudy A, Vavasseur A, Hosity E, Dreyer I, Leonhardt N, Thibaud JB, Véry AA, Simonneau T,  
971 Sentenac H** (2008) Plant adaptation to fluctuating environment and biomass production  
972 are strongly dependent on guard cell potassium channels. *Proc Natl Acad Sci U S A* **105**:  
973 5271–5276
- 974 **Lee DW, Kim SJ, Oh YJ, Choi B, Lee J, Hwang I** (2016) Arabidopsis BAG1 Functions as a Cofactor  
975 in Hsc70-Mediated Proteasomal Degradation of Unimported Plastid Proteins. *Mol Plant* **9**:  
976 1428–1431
- 977 **Lefoulon C, Waghmare S, Karnik R, Blatt MR** (2018) Gating control and K. *Plant Cell Env* **41**:  
978 2668–2677
- 979 **Li K, Jiang Q, Bai X, Yang YF, Ruan MY, Cai SQ** (2017) Tetrameric Assembly of K<sup>+</sup> Channels  
980 Requires ER-Located Chaperone Proteins. *Mol Cell* **65**: 52–65
- 981 **Long SB, Campbell EB, Mackinnon R** (2005) Crystal structure of a mammalian voltage-  
982 dependent Shaker family K<sup>+</sup> channel. *Science* (80- ) **309**: 897–903
- 983 **Mäser P, Thomine S, Schroeder JI, Ward JM, Hirschi K, Sze H, Talke IN, Amtmann A, Maathuis  
984 FJ, Sanders D, et al** (2001) Phylogenetic relationships within cation transporter families of  
985 Arabidopsis. *Plant Physiol* **126**: 1646–1667
- 986 **Matheson LA, Hanton SL, Brandizzi F** (2006) Traffic between the plant endoplasmic reticulum  
987 and Golgi apparatus: to the Golgi and beyond. *Curr Opin Plant Biol* **9**: 601–609
- 988 **Meckel T, Hurst AC, Thiel G, Homann U** (2004) Endocytosis against high turgor: intact guard  
989 cells of *Vicia faba* constitutively endocytose fluorescently labelled plasma membrane and  
990 GFP-tagged K-channel KAT1. *Plant J* **39**: 182–193
- 991 **Merlot S, Mustilli AC, Genty B, North H, Lefebvre V, Sotta B, Vavasseur A, Giraudat J** (2002)

- 992 Use of infrared thermal imaging to isolate Arabidopsis mutants defective in stomatal  
993 regulation. *Plant J* **30**: 601–609
- 994 **Mumberg D, Müller R, Funk M** (1994) Regulatable promoters of *Saccharomyces cerevisiae*:  
995 comparison of transcriptional activity and their use for heterologous expression. *Nucleic*  
996 *Acids Res* **22**: 5767–5768
- 997 **Nakamura RL, McKendree WL, Hirsch RE, Sedbrook JC, Gaber RF, Sussman MR** (1995)  
998 Expression of an Arabidopsis potassium channel gene in guard cells. *Plant Physiol* **109**:  
999 371–374
- 1000 **Navarrete C, Petrezselyova S, Barreto L, Martinez JL, Zahradka J, Arino J, Sychrova H, Ramos J**  
1001 (2010) Lack of main K plus uptake systems in *Saccharomyces cerevisiae* cells affects yeast  
1002 performance in both potassium-sufficient and potassium-limiting conditions. *FEMS Yeast*  
1003 *Res* **10**: 508–517
- 1004 **Obrdlik P, El-Bakkoury M, Hamacher T, Cappellaro C, Vilarino C, Fleischer C, Ellerbrok H,**  
1005 **Kamuzinzi R, Ledent V, Blaudez D, et al** (2004) K+ channel interactions detected by a  
1006 genetic system optimized for systematic studies of membrane protein interactions. *Proc*  
1007 *Natl Acad Sci* **101**: 12242–7
- 1008 **Pardo JM, Quintero FJ** (2002) Plants and sodium ions: keeping company with the enemy.  
1009 *Genome Biol* **3**: doi:10.1186/gb-2002-3-6-reviews1017
- 1010 **Paumi CM, Menendez J, Arnoldo A, Engels K, Iyer KR, Thaminy S, Georgiev O, Barral Y,**  
1011 **Michaelis S, Stagljar I** (2007) Mapping protein-protein interactions for the yeast ABC  
1012 transporter Ycf1p by integrated split-ubiquitin membrane yeast two-hybrid analysis. *Mol*  
1013 *Cell* **26**: 15–25
- 1014 **Pilot G, Pratelli R, Gaymard F, Meyer Y, Sentenac H** (2003) Five-group distribution of the  
1015 Shaker-like K+ channel family in higher plants. *J Mol Evol* **56**: 418–434
- 1016 **Planes MD, Niñoles R, Rubio L, Bissoli G, Bueso E, García-Sánchez MJ, Alejandro S, Gonzalez-**  
1017 **Guzmán M, Hedrich R, Rodriguez PL, et al** (2015) A mechanism of growth inhibition by  
1018 abscisic acid in germinating seeds of *Arabidopsis thaliana* based on inhibition of plasma  
1019 membrane H+-ATPase and decreased cytosolic pH, K+, and anions. *J Exp Bot* **66**: 813–825
- 1020 **Prokhnevsky AI, Peremyslov V V., Dolja V V.** (2005) Actin Cytoskeleton Is Involved in Targeting  
1021 of a Viral Hsp70 Homolog to the Cell Periphery. *J Virol* **79**: 14421–14428
- 1022 **Rodríguez-Navarro A** (2000) Potassium transport in fungi and plants. *Biochim Biophys Acta*  
1023 **1469**: 1–30
- 1024 **Ronzier E, Corratgé-Faillie C, Sanchez F, Prado K, Brière C, Leonhardt N, Thibaud JB, Xiong TC**  
1025 (2014) CPK13, a noncanonical Ca<sup>2+</sup>-dependent protein kinase, specifically inhibits KAT2  
1026 and KAT1 shaker K+ channels and reduces stomatal opening. *Plant Physiol* **166**: 314–326
- 1027 **Saponaro A, Porro A, Chaves-Sanjuan A, Nardini M, Rauh O, Thiel G, Moroni A** (2017)  
1028 Fusicoccin Activates KAT1 Channels by Stabilizing Their Interaction with 14-3-3 Proteins.  
1029 *Plant Cell* **29**: 2570–2580
- 1030 **Sarrion-Perdigones A, Vazquez-Vilar M, Palací J, Castelijns B, Forment J, Ziarsolo P, Blanca J,**  
1031 **Granell A, Orzaez D** (2013) GoldenBraid 2.0: a comprehensive DNA assembly framework  
1032 for plant synthetic biology. *Plant Physiol* **162**: 1618–1631

- 1033 **Sato A, Sato Y, Fukao Y, Fujiwara M, Umezawa T, Shinozaki K, Hibi T, Taniguchi M, Miyake H,**  
1034 **Goto DB, et al** (2009) Threonine at position 306 of the KAT1 potassium channel is  
1035 essential for channel activity and is a target site for ABA-activated SnRK2/OST1/SnRK2.6  
1036 protein kinase. *Biochem J* **424**: 439–448
- 1037 **Schachtman DP, Schroeder JI, Lucas WJ, Anderson JA, Gaber RF** (1992) Expression of an  
1038 inward-rectifying potassium channel by the Arabidopsis KAT1 cDNA. *Science* (80- ) **258**:  
1039 1654–1658
- 1040 **Sessions A, Burke E, Presting G, Aux G, McElver J, Patton D, Dietrich B, Ho P, Bacwaden J, Ko**  
1041 **C, et al** (2002) A high-throughput Arabidopsis reverse genetics system. *Plant Cell* **14**:  
1042 2985–2994
- 1043 **Sieben C, Mikosch M, Brandizzi F, Homann U** (2008) Interaction of the K(+)-channel KAT1 with  
1044 the coat protein complex II coat component Sec24 depends on a di-acidic endoplasmic  
1045 reticulum export motif. *Plant J* **56**: 997–1006
- 1046 **Sottocornola B, Gazzarrini S, Olivari C, Romani G, Valbuzzi P, Thiel G, Moroni A** (2008) 14-3-3  
1047 proteins regulate the potassium channel KAT1 by dual modes. *Plant Biol* **10**: 231–236
- 1048 **Sottocornola B, Visconti S, Orsi S, Gazzarrini S, Giacometti S, Olivari C, Camoni L, Aducci P,**  
1049 **Marra M, Abenavoli A, et al** (2006) The potassium channel KAT1 is activated by plant and  
1050 animal 14-3-3 proteins. *J Biol Chem* **281**: 35735–35741
- 1051 **Sutter JU, Campanoni P, Tyrrell M, Blatt MR** (2006) Selective mobility and sensitivity to  
1052 SNAREs is exhibited by the Arabidopsis KAT1 K<sup>+</sup> channel at the plasma membrane. *Plant*  
1053 *Cell* **18**: 935–954
- 1054 **Sutter JU, Sieben C, Hartel A, Eisenach C, Thiel G, Blatt MR** (2007) Abscisic acid triggers the  
1055 endocytosis of the arabidopsis KAT1 K<sup>+</sup> channel and its recycling to the plasma  
1056 membrane. *Curr Biol* **17**: 1396–1402
- 1057 **Szyroki A, Ivashikina N, Dietrich P, Roelfsema MR, Ache P, Reintanz B, Deeken R, Godde M,**  
1058 **Felle H, Steinmeyer R, et al** (2001) KAT1 is not essential for stomatal opening. *Proc Natl*  
1059 *Acad Sci U S A* **98**: 2917–2921
- 1060 **Takayama S, Reed JC** (2001) Molecular chaperone targeting and regulation by BAG family  
1061 proteins. *Nat Cell Biol* **3**: doi:10.1038/ncb1001-e237
- 1062 **Véry AA, Gaymard F, Bosseux C, Sentenac H, Thibaud JB** (1995) Expression of a cloned plant  
1063 K<sup>+</sup> channel in *Xenopus* oocytes: analysis of macroscopic currents. *Plant J* **7**: 321–332
- 1064 **Véry AA, Sentenac H** (2003) Molecular mechanisms and regulation of K<sup>+</sup> transport in higher  
1065 plants. *Annu Rev Plant Biol* **54**: 575–603
- 1066 **Wang Y, Hills A, Blatt MR** (2014) Systems analysis of guard cell membrane transport for  
1067 enhanced stomatal dynamics and water use efficiency. *Plant Physiol* **164**: 1593–1599
- 1068 **Wang Y, Holroyd G, Hetherington AM, Ng CKY** (2004) Seeing “cool” and “hot” - Infrared  
1069 thermography as a tool for non-invasive, high-throughput screening of Arabidopsis guard  
1070 cell signalling mutants. *J Exp Bot* **55**: 1187–1193
- 1071 **Williams B, Kabbage M, Britt R, Dickman MB** (2010) AtBAG7, an Arabidopsis Bcl-2-associated  
1072 athanogene, resides in the endoplasmic reticulum and is involved in the unfolded protein  
1073 response. *Proc Natl Acad Sci* **107**: 6088–6093

- 1074 **Winter D, Vinegar B, Nahal H, Ammar R, Wilson G V, Provart NJ** (2007) An “Electronic  
1075 Fluorescent Pictograph” browser for exploring and analyzing large-scale biological data  
1076 sets. *PLoS One* **2**: e718
- 1077 **Wu HY, Liu KH, Wang YC, Wu JF, Chiu WL, Chen CY, Wu SH, Sheen J, Lai EM** (2014) AGROBEST:  
1078 an efficient Agrobacterium-mediated transient expression method for versatile gene  
1079 function analyses in Arabidopsis seedlings. *Plant Methods* **10**: 19
- 1080 **Xicluna J, Lacombe B, Dreyer I, Alcon C, Jeanguenin L, Sentenac H, Thibaud JB, Chérel I** (2007)  
1081 Increased functional diversity of plant K<sup>+</sup> channels by preferential heteromerization of  
1082 the shaker-like subunits AKT2 and KAT2. *J Biol Chem* **282**: 486–494
- 1083 **Yan A, Wu E, Lennarz WJ** (2005) Studies of yeast oligosaccharyl transferase subunits using the  
1084 split-ubiquitin system: topological features and in vivo interactions. *Proc Natl Acad Sci U S*  
1085 *A* **102**: 7121–7126
- 1086 **Yang Y, Costa A, Leonhardt N, Siegel RS, Schroeder JI** (2008) Isolation of a strong Arabidopsis  
1087 guard cell promoter and its potential as a research tool. *Plant Methods* **4**: 6
- 1088 **Young JC** (2014) The role of the cytosolic HSP70 chaperone system in diseases caused by  
1089 misfolding and aberrant trafficking of ion channels. *Dis Model Mech* **7**: 319–329
- 1090 **Zhang B, Karnik R, Waghmare S, Donald N, Blatt MR** (2017) VAMP721 Conformations Unmask  
1091 an Extended Motif for K<sup>+</sup> Channel Binding and Gating Control. *Plant Physiol* **173**: 536–551
- 1092 **Zhang B, Karnik R, Wang Y, Wallmeroth N, Blatt MR, Grefen C** (2015) The Arabidopsis R-  
1093 SNARE VAMP721 Interacts with KAT1 and KC1 K<sup>+</sup> Channels to Moderate K<sup>+</sup> Current at the  
1094 Plasma Membrane. *Plant Cell* **27**: 1697–1717
- 1095

**A****B****C**

**Figure 1. Effect of the co-expression of interacting proteins on the functional complementation by KAT1 in yeast.** A) The indicated plasmids were co-transformed in the *trk1 trk2* mutant strain (PLY240) and the growth of the strains was assayed as described in Materials and Methods using the Translucent media (which contains 12  $\mu$ M potassium) with or without methionine supplementation to decrease the expression of KAT1 (under control of the MET25 promoter). The graph shows the average value of the optical density at 72 hours for triplicate determinations and the experiment was done with at least 3 independent transformants for each plasmid combination. (Translucent media with no KCl supplementation = Low KCl (12  $\mu$ M K<sup>+</sup>); Translucent media containing 0.75 mg/mL methionine = Low KAT1; Translucent media + 50 mM KCl added = High KCl; Translucent media +/- KCl without methionine = High KAT1). B) Immunoblot analysis of protein extracts from the indicated strains showing the correct expression of each of the fusion proteins. The KAT1 bait vector protein is detected with the anti-LexA antibody and the prey proteins with the anti-HA antibody. Results for a representative clone are shown. The long exposure is included to visualize the expression of the RPT2 prey protein, which accumulates less than the other two prey proteins. Data presented are the mean  $\pm$ SD and similar results were observed for three independent transformants. Asterisks (\*\*) indicate statistical significance (Student t test) with a p value < 0.01. C) The KAT1 signal and the corresponding loading control were quantified using the ImageJ software and the average values of KAT1/loading control (Normalized KAT1) was calculated for 6 control strains (KAT1\_empty vector) and 7 KAT1\_BAG4 strains. Data presented are the mean  $\pm$ SD.

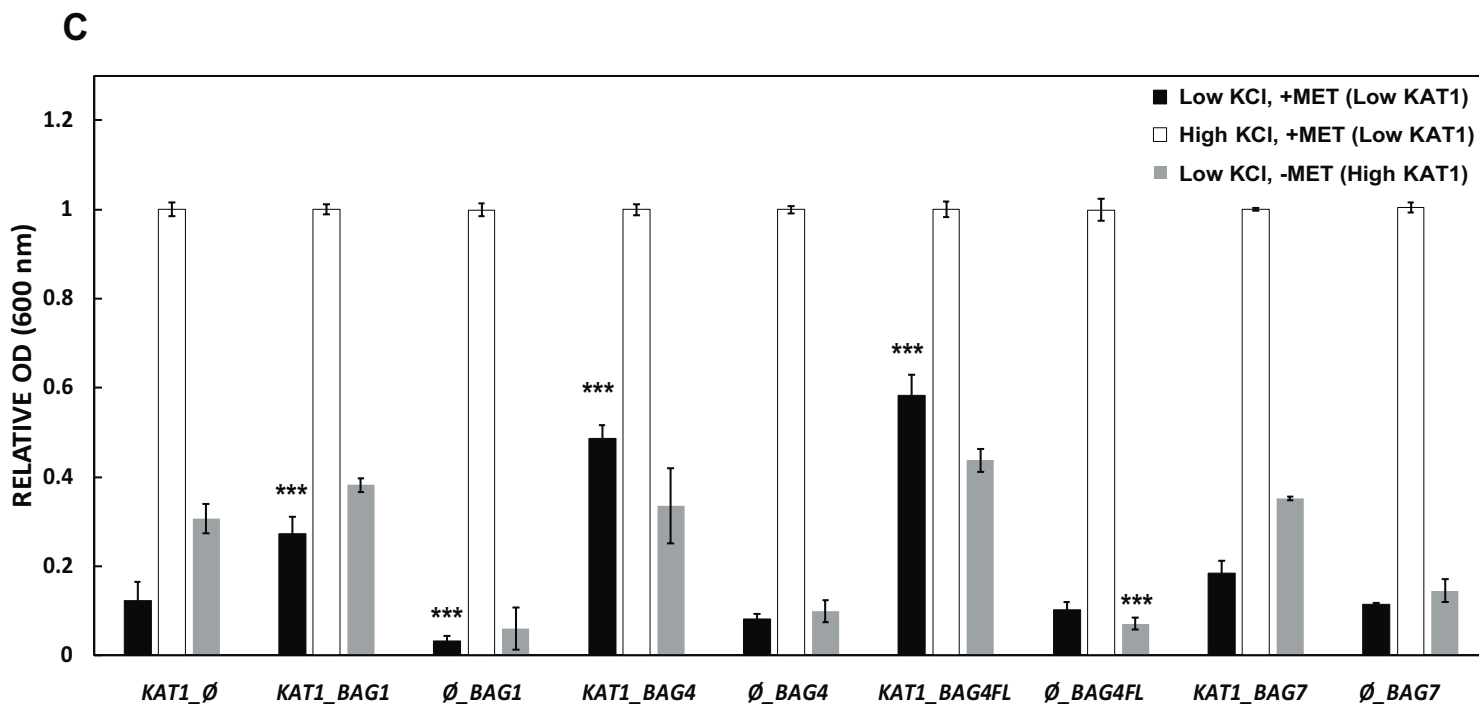
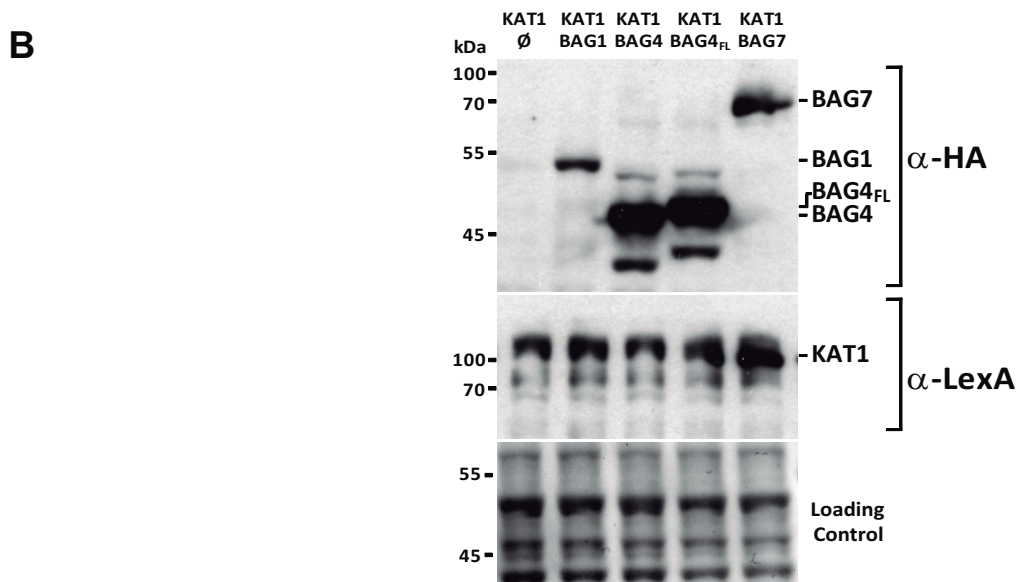
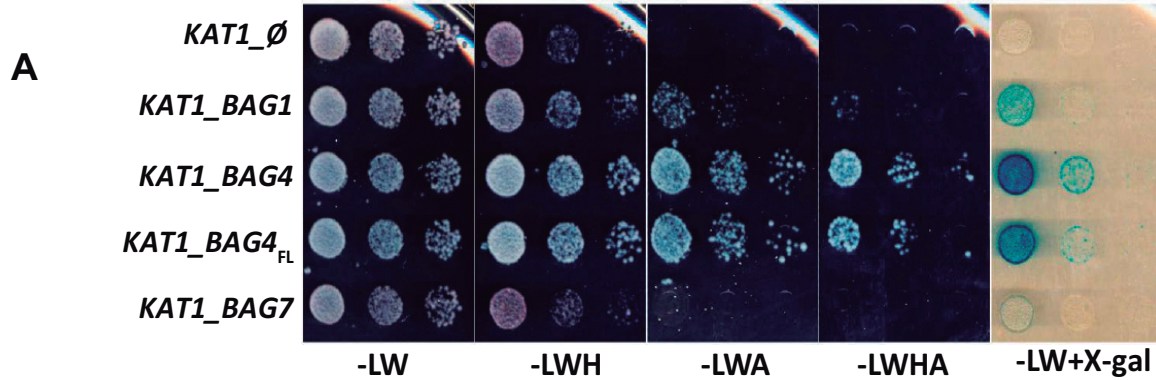


Figure 2. Study of the specificity of the interaction between KAT1 and other BAG family members. A) The indicated plasmids were transformed into the THY.AP4 strain and grown to saturation in selective media. Serial dilutions were spotted onto media with the indicated composition to test for the protein-protein interaction between KAT1 and the indicated BAG family proteins. Identical results were observed for four independent clones. B) Immunoblot analysis of protein extracts from the indicated strains showing the correct expression of each of the fusion proteins. The KAT1 bait protein is detected with the anti-LexA antibody and the prey proteins with the anti-HA antibody. Results for a representative clone are shown. C) The indicated plasmids were co-transformed in the *trk1 trk2* mutant strain (PLY240) and the growth of the strains was assayed as described in Figure 1A. The average value of triplicate determinations of the optical density of the growth normalized to the potassium supplemented media is shown for each strain. Similar results were observed for 3 independent clones of each plasmid combination. Asterisks (\*\*\*) indicate statistical significance (Student t test) with a p value < 0.001 compared to the *KAT1\_∅* strain.



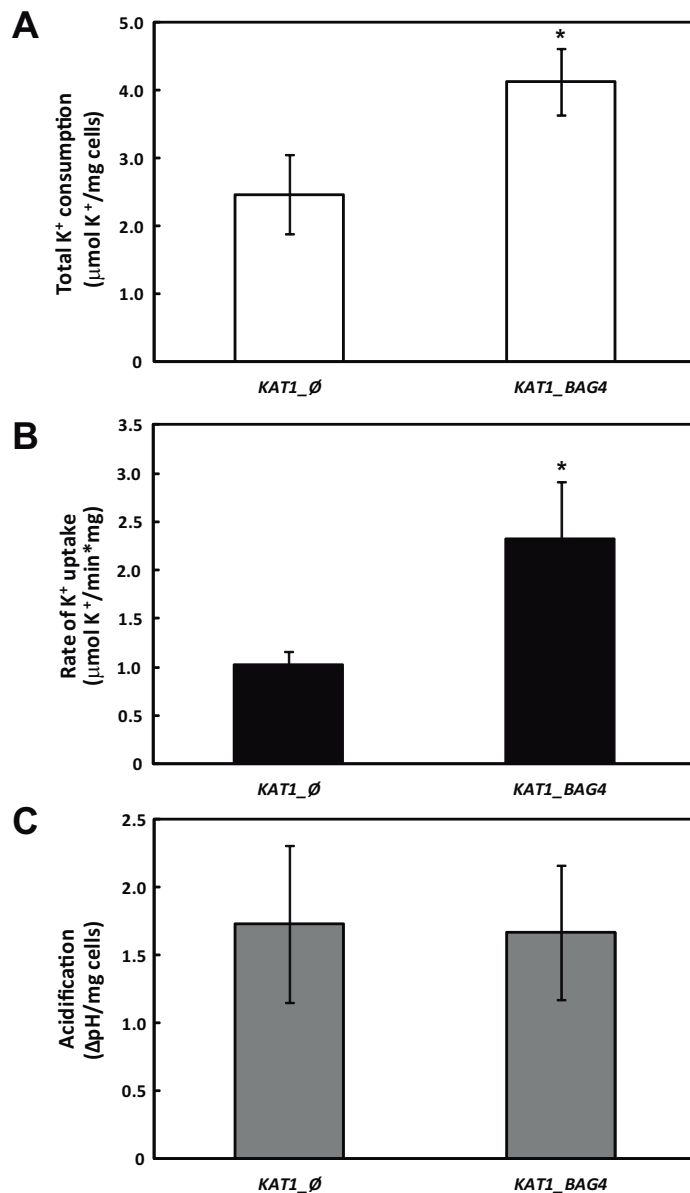


Figure 3. Potassium uptake and external acidification. The indicated plasmids were co-transformed in the *trk1 trk2* mutant strain (PLY240) and the strains were grown in low KCl and low KAT1 conditions and processed as described in Materials and Methods. A) The bars represent the average value for three independent experiments for the total potassium uptake for 45 minutes expressed as  $\mu\text{mol K}^+/\text{mg cells}$ . B) The bars represent the average value for three independent experiments for the rate of potassium uptake expressed as  $\mu\text{mol K}^+/\text{min}\cdot\text{mg cells}$  calculated using the slope of the depletion curve normalized to the wet weight of the cells. C) The bars represent the average value for three independent experiments of the change in the pH value measured in parallel with the potassium consumption. The change in the external pH was determined during the first 15 minutes after glucose addition and was normalized to the wet weight of the cells. Asterisks (\*) indicate statistical significance (Student t test) with a p value < 0.05.

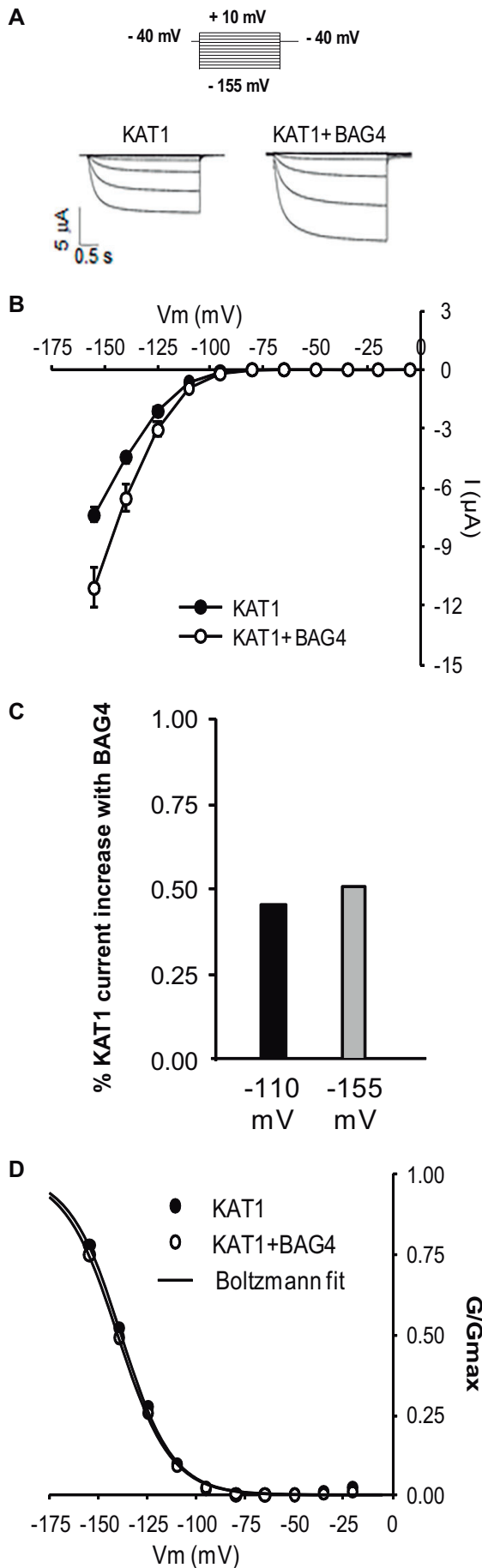
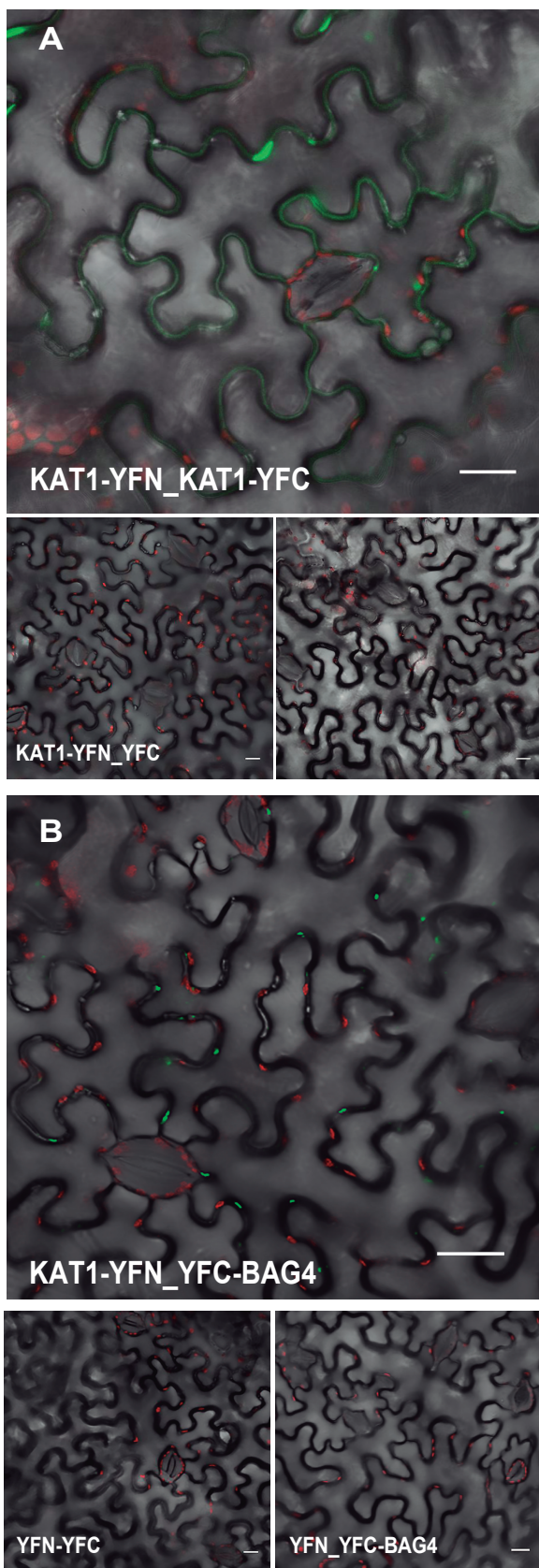
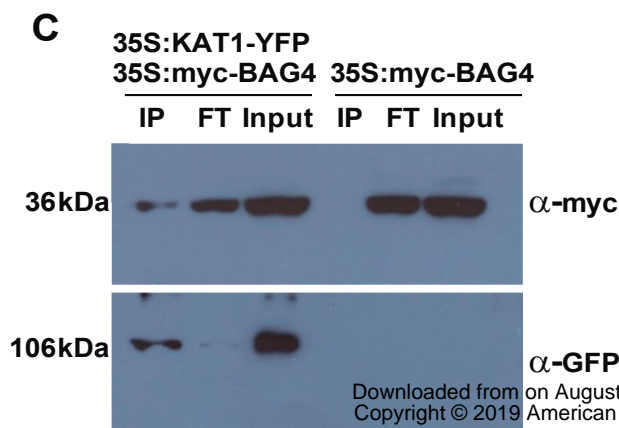
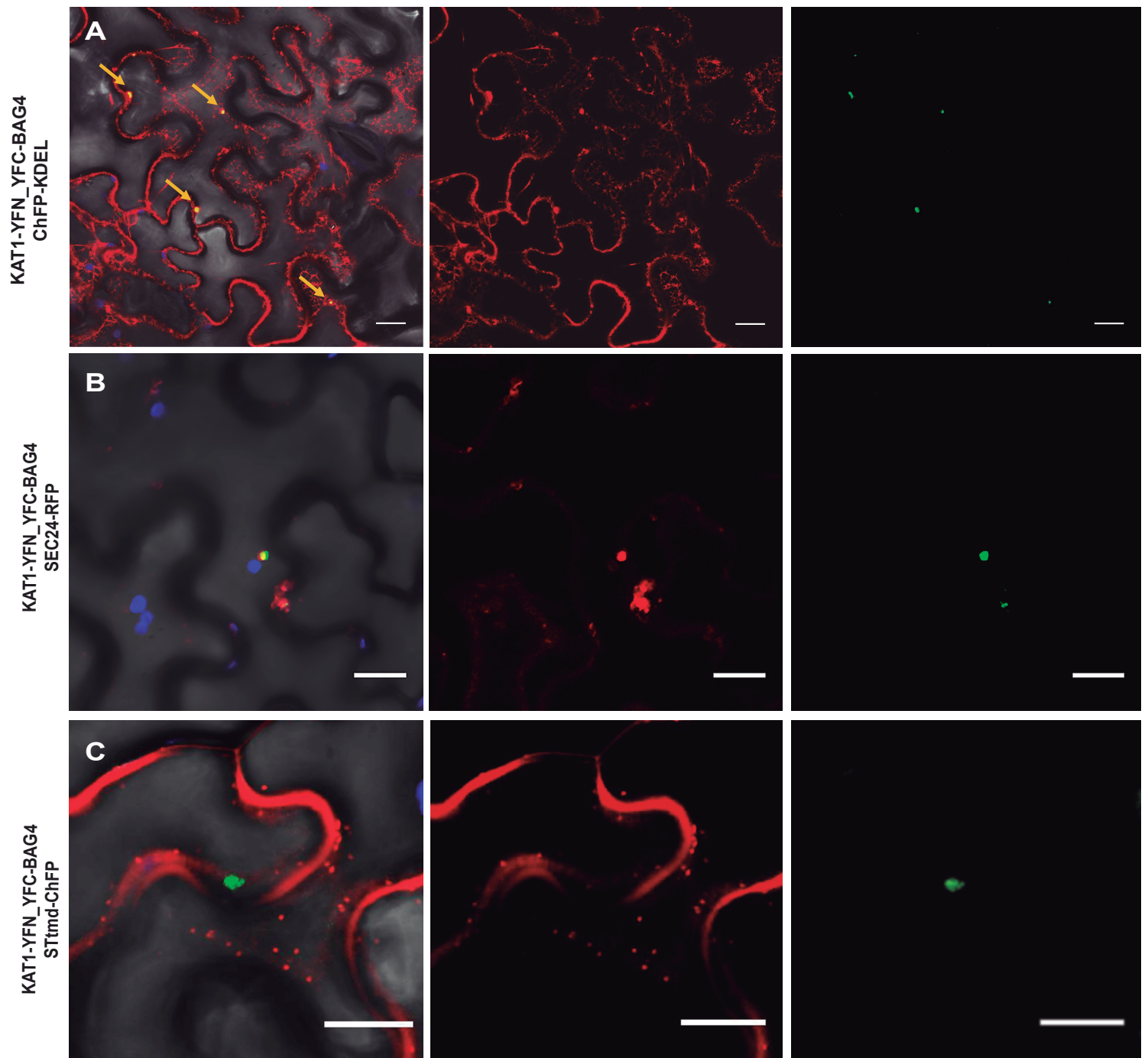


Figure 4. BAG4 co-expression increases KAT1 current in *Xenopus* oocytes. A) Voltage-clamp protocol and representative current traces recorded by two-electrode voltage clamp in the presence of 100 mM KCl on oocytes co-expressing KAT1 or KAT1 and BAG4. B) KAT1 current ( $I$ ) –voltage ( $V$ ) relationships of oocytes co-expressing KAT1 and BAG4 (white circles) or expressing KAT1 alone (black circles). Data are means  $\pm$  SE ( $n=7$  for KAT1,  $n=11$  for KAT1 + BAG4), and are representative of two experiments performed on different oocyte batches. C) Increase of mean KAT1 current upon BAG4 co-expression, at  $-110$  mV (black) and at  $-155$  mV (grey). Mean currents are from B). D) Voltage-dependence of KAT1-current activation in the presence of BAG4 (white circles) or with KAT1 expressed alone (black circles). Gating parameters ( $z$ , gating charge, and  $E_{a50}$ , half-activation potential) were estimated by performing fits to the KAT1  $I$ - $V$  relationships (in the presence or absence of BAG4) (Baudry et al., 2010). G, KAT1 macroscopic conductance ( $G = I/V$ );  $G_{max}$ , KAT1 macroscopic conductance at infinitely negative voltage.



**Figure 5. Confirmation of the interaction between KAT1 and BAG4 in *N. benthamiana*.** Agrobacterium strains harbouring the indicated plasmids were used to infiltrate *N. benthamiana* leaves and images were obtained using fluorescence confocal microscopy 72 hours post-infiltration. A) Representative BiFC images for the KAT1-KAT1 interaction and control plasmids. The overlay of the grey scale and BiFC fluorescence is shown. Leaf epithelial cells and stomata are visible. B) Representative BiFC images for the KAT1-BAG4 interaction. Representative images of the experiments performed with the control plasmids are shown below. The red signal corresponds to chloroplast autofluorescence. For panels A and B, similar results were observed in at least four independent experiments performed on different days. (Bar = 20 $\mu$ m) C) Agrobacterium strains expressing the indicated plasmids were used to infiltrate *N. benthamiana* leaves. Samples were taken at 72 hours post-infiltration and processed for protein extraction and co-immunoprecipitation as described in Materials and Methods. The figure shows the results of the immunodetection using antibodies that recognize the BAG4 and KAT1 proteins. The amount of BAG4 recovered in the KAT1 purification is shown in the first lane on the left. Similar results were observed in two independent experiments performed on different days. (YFN = N-terminal part of YFP; YFC=C-terminal part of YFP; IP=immunoprecipitation; FT=flow through).





**Figure 6. The KAT1-BAG4 complex co-localizes with the ER and ERES markers.**

A) A plasmid containing the KAT1-BAG4 BiFC interaction and the ER marker ChFP-KDEL were infiltrated as described. The BiFC signal (right), ChFP signal (center), and the overlay image of the grey scale, BiFC fluorescence and the ChFP signals (left) are shown. Leaf epithelial cells and stomata are visible. B and C) The same co-localization analysis of the KAT1-BAG4 complex was performed with the ER exit site marker, Sec24 fused to RFP (Sec24-RFP) (B) and the STtmd-ChFP Golgi marker (C). The yellow arrows indicate the points of co-localization with the ER marker. Chloroplast autofluorescence is shown in blue. (Bar = 20 $\mu$ m). (YFN = N-terminal part of YFP; YFC=C-terminal part of YFP; ChFP= Cherry Fluorescent Protein; RFP=Red Fluorescent Protein; STtmd-ChFP= rat  $\alpha$ -2,6-sialyltransferase transmembrane domain fused to the Cherry fluorescent protein).

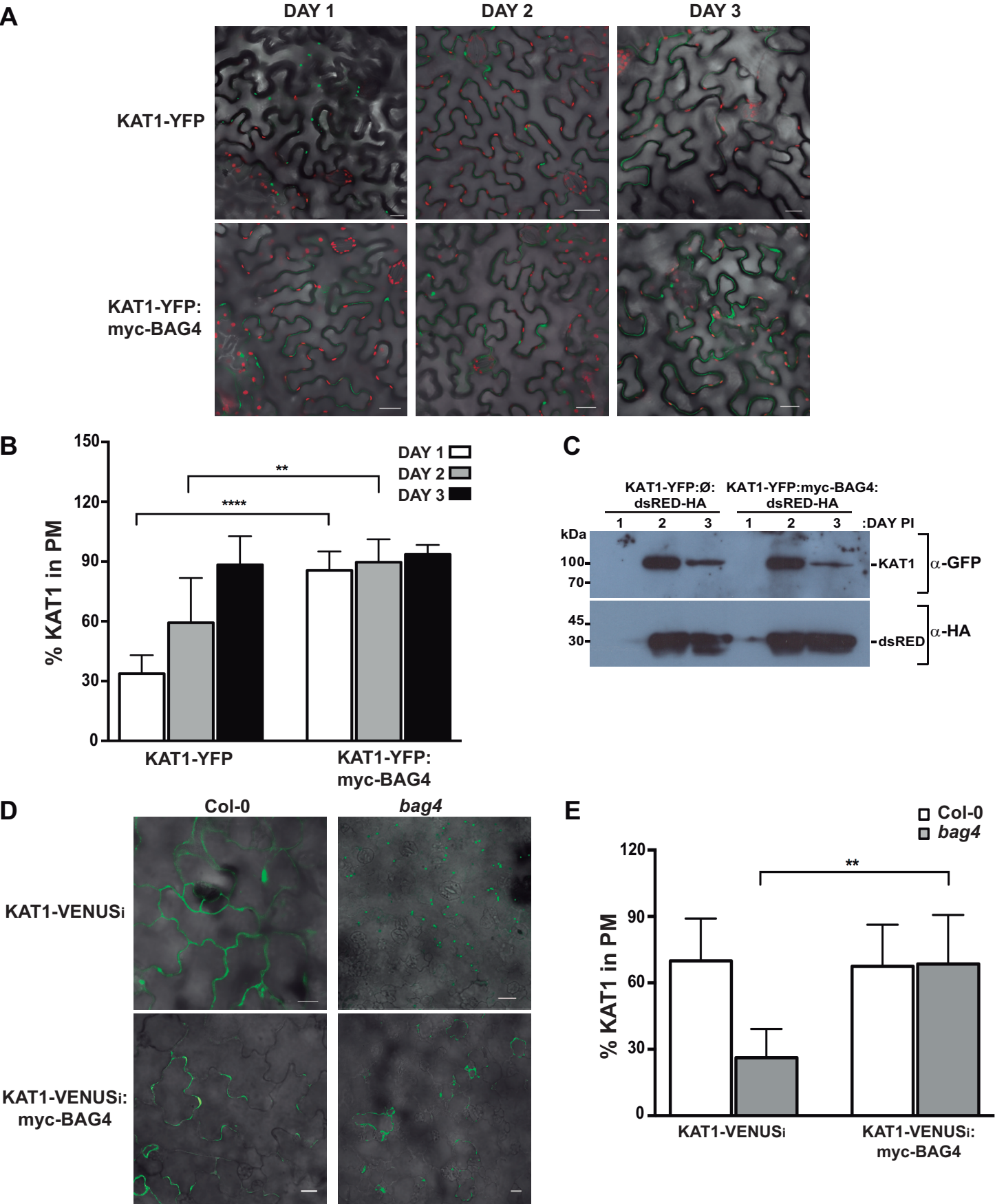


Figure 7. BAG4 expression effects the subcellular localization of KAT1. A) Plasmids containing KAT1-YFP or both KAT1-YFP and BAG4 were transiently expressed in *N. benthamiana* using agro-infiltration. The fluorescence signal was analyzed by confocal microscopy days 1, 2 and 3 days post-infiltration. Representative images are shown. Similar results were observed in three independent experiments. B) The percentage of the fluorescence signal present in the plasma membrane was quantified using ImageJ, as described in Materials and Methods. The graph shows the average values  $\pm$ SD for 10 cells for each condition tested. C) Similar experiments as described in part a) were performed, but using GoldenBraid plasmids containing KAT1-YFP:dsRED-HA or KAT1-YFP:myc-BAG4:dsRED-HA. Whole cell extracts were prepared from infiltrated areas (previously confirmed to express KAT1-YFP) and proteins were processed for immunodetection. The dsRED-HA protein serves as an internal control for the efficiency of transient expression. D) The KAT1-VENUSintron (KAT1-VENUSi, top row) or the KAT1-VENUSintron\_BAG4 (bottom row) plasmids were transiently expressed in the Col-0 and the bag4 mutant Arabidopsis lines using agro-infiltration. The fluorescence signal was analyzed by confocal microscopy 2 days after infiltration. Representative images are shown and similar results were observed in three independent experiments. (Bar = 20 $\mu$ m) E) The percentage of the fluorescence signal present in the plasma membrane was quantified using ImageJ, as described in Materials and Methods. The graph shows the average values  $\pm$ SD for 10 cells for each condition tested. Copyright © 2019 American Society of Plant Biologists. All rights reserved.

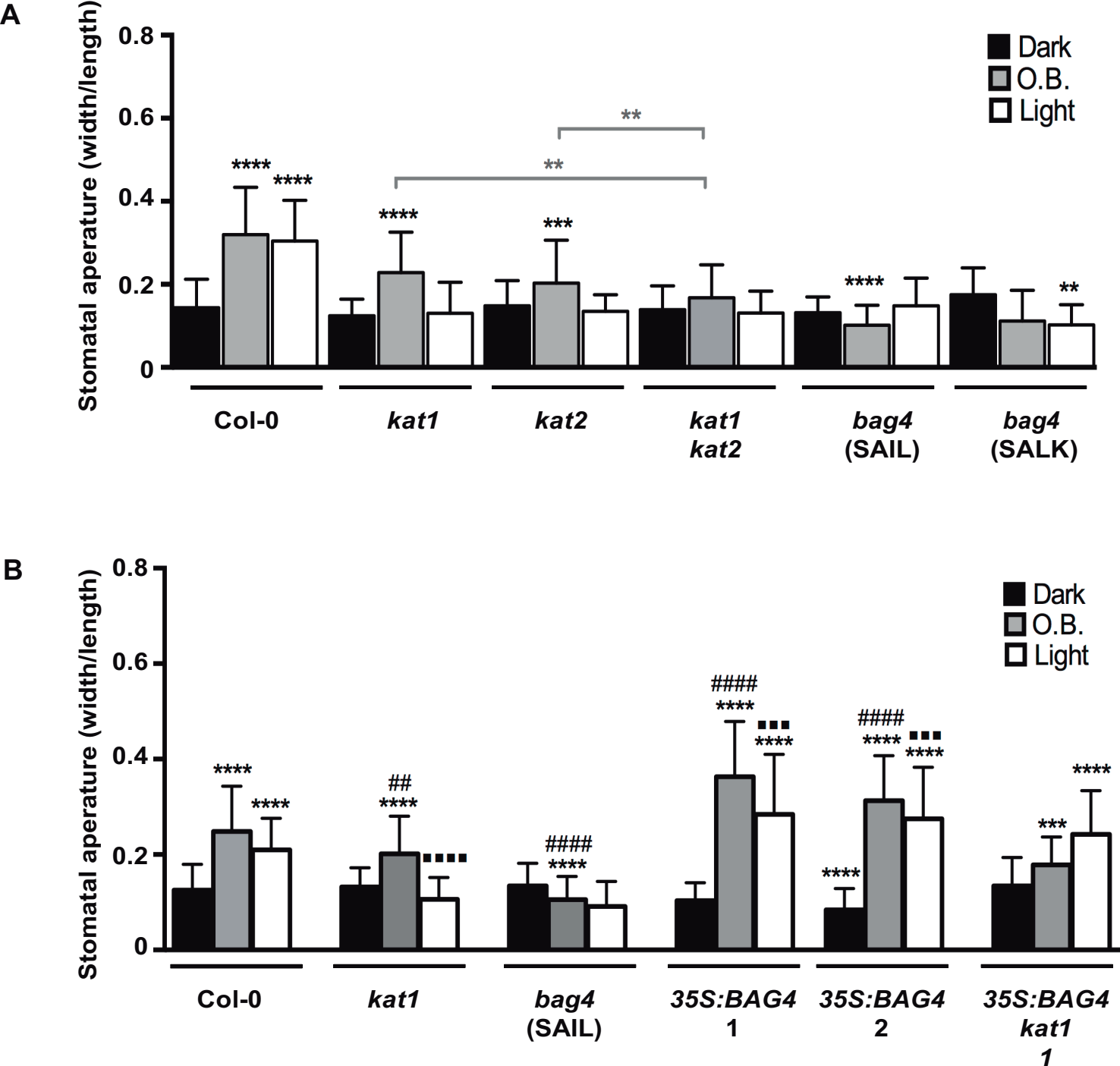


Figure 8. Effect of BAG4 loss and gain-of-function on stomatal aperture. Stomata from the indicated *Arabidopsis* lines were analyzed as described in Materials and Methods. The data show the average ratio for 60-100 stomata and the error bars represent the standard deviation. A) The width/length ratio of stomata of the different mutant lines were determined in leaves from the indicated lines harvested 1 hour before the lights turned on (Dark), incubated for 2.5 hours in opening buffer in the dark (Opening buffer, O.B.) or 2.5 hours after the lights turned on (Light). Similar results were observed in three independent experiments. B) The width/length ratio of stomata of control lines and Col-0 and *kat1* homozygous for 35S:BAG4 transgene were determined as described in A. For both experiments, the asterisks indicate statistical significance as compared to the Col-0 dark control (Student t test) (\*\*: p value < 0.01; \*\*\*: p value < 0.001; \*\*\*\*: p value < 0.0001). The length/width ratio was also significantly increased in BAG4 overexpressing lines in both light and opening buffer (# indicates statistical comparison with Col-0 O.B. and • indicates statistical comparison with Col-0 light).

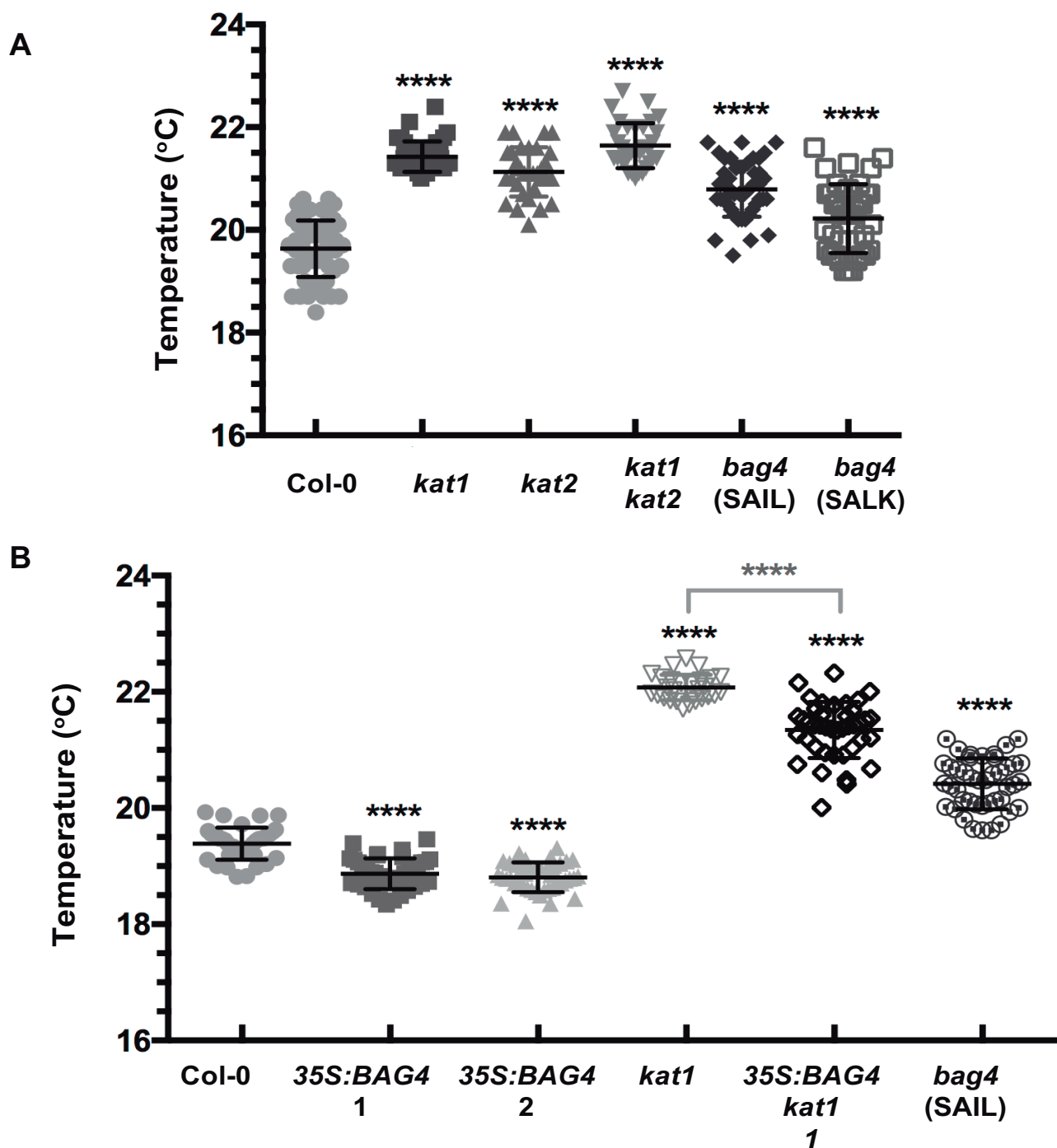


Figure 9. Effect of BAG4 loss and gain-of-function on leaf temperature. The same lines described in Figure 7 were analyzed for leaf temperature using an infrared thermography, as described in Materials and Methods (Panel A mutant lines, Panel B control and 35S:BAG4 lines). Each symbol represents an individual measurement and the bar represents the average value for 10 measurements of 6 different plants for each genotype. The error bars represent the standard deviation. For both experiments, the asterisks indicate statistical significance as compared to the Col-0 control or the comparisons indicated by the brackets above the graphs (Student t-test)

(\*\* : p value < 0.01; \*\*\* : p value < 0.001; \*\*\*\* p value < 0.0001).

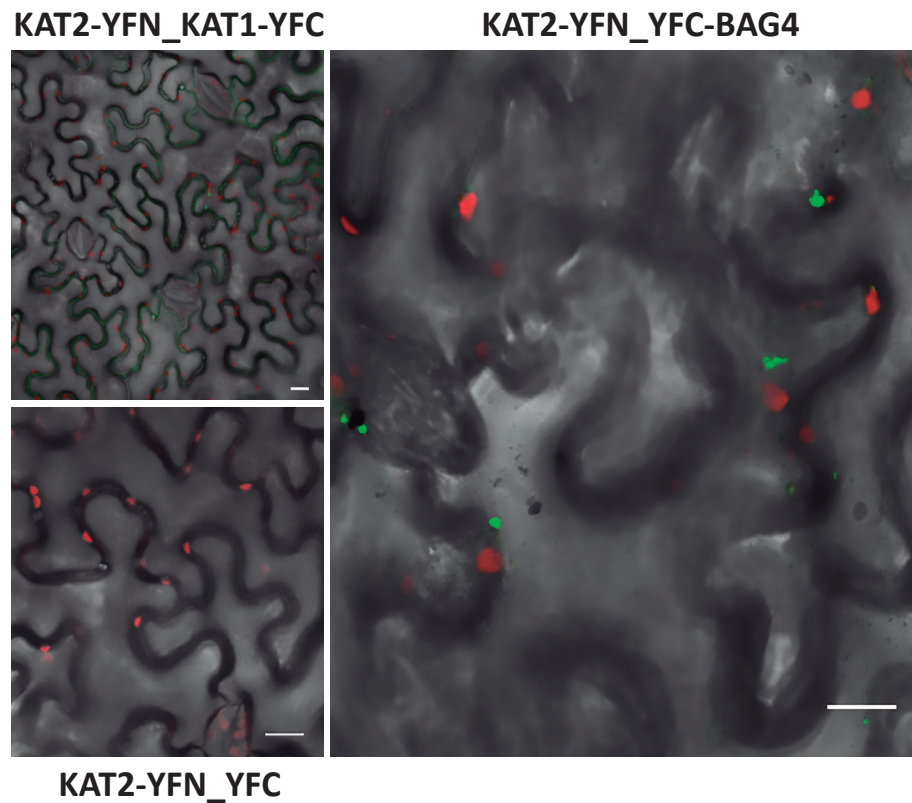


Figure 10. BAG4 interacts with KAT2 in BiFC assays in *N. benthamiana*. Interaction assays were carried out and analyzed as described in the legend to Figure 5. As shown, a similar pattern of interaction is observed for KAT2 when tested with BAG4 (compare with Figure 5B). In this image, the BiFC signals corresponding to the KAT2-KAT1 and KAT2-BAG4 interactions are shown in green and the chloroplast autofluorescence is shown in red. (Bar = 20 $\mu$ m)



## Parsed Citations

**Anderson JA, Huprikar SS, Kochian L V, Lucas WJ, Gaber RF (1992) Functional expression of a probable *Arabidopsis thaliana* potassium channel in *Saccharomyces cerevisiae*. Proc Natl Acad Sci U S A 89: 3736–3740**

Pubmed: [Author and Title](#)

Google Scholar: [Author Only](#) [Title Only](#) [Author and Title](#)

**Bertl A, Ramos J, Ludwig J, Lichtenberg-Fraté H, Reid J, Bihler H, Calero F, Martínez P, Ljungdahl PO (2003) Characterization of potassium transport in wild-type and isogenic yeast strains carrying all combinations of *trk1*, *trk2* and *tok1* null mutations. 47: 767–780**

Pubmed: [Author and Title](#)

Google Scholar: [Author Only](#) [Title Only](#) [Author and Title](#)

**Doukhanina E V., Chen S, Van Der Zalm E, Godzik A, Reed J, Dickman MB (2006) Identification and functional characterization of the BAG protein family in *Arabidopsis thaliana*. J Biol Chem. doi: 10.1074/jbc.M511794200**

Pubmed: [Author and Title](#)

Google Scholar: [Author Only](#) [Title Only](#) [Author and Title](#)

**Dreyer I, Antunes S, Hoshi T, Müller-Röber B, Palme K, Pongs O, Reintanz B, Hedrich R (1997) Plant K<sup>+</sup> channel alpha-subunits assemble indiscriminately. Biophys J 72: 2143–2150**

Pubmed: [Author and Title](#)

Google Scholar: [Author Only](#) [Title Only](#) [Author and Title](#)

**Duby G, Hosy E, Fizames C, Alcon C, Costa A, Sentenac H, Thibaud JB (2008) AtKC1, a conditionally targeted Shaker-type subunit, regulates the activity of plant K<sup>+</sup> channels. Plant J 53: 115–123**

Pubmed: [Author and Title](#)

Google Scholar: [Author Only](#) [Title Only](#) [Author and Title](#)

**Dunn KW, Kamocka MM, McDonald JH (2011) A practical guide to evaluating colocalization in biological microscopy. Am J Physiol Cell Physiol 300: C723–42**

Pubmed: [Author and Title](#)

Google Scholar: [Author Only](#) [Title Only](#) [Author and Title](#)

**Eisenach C, Chen ZH, Grefen C, Blatt MR (2012) The trafficking protein SYP121 of *Arabidopsis* connects programmed stomatal closure and K<sup>+</sup> channel activity with vegetative growth. Plant J 69: 241–251**

Pubmed: [Author and Title](#)

Google Scholar: [Author Only](#) [Title Only](#) [Author and Title](#)

**Gierth M, Mäser P (2007) Potassium transporters in plants – Involvement in K<sup>+</sup> acquisition, redistribution and homeostasis. 581: 2348–2356**

Pubmed: [Author and Title](#)

Google Scholar: [Author Only](#) [Title Only](#) [Author and Title](#)

**Grefen C, Chen Z, Honsbein A, Donald N, Hills A, Blatt MR (2010) A novel motif essential for SNARE interaction with the K(+) channel KC1 and channel gating in *Arabidopsis*. Plant Cell 22: 3076–3092**

Pubmed: [Author and Title](#)

Google Scholar: [Author Only](#) [Title Only](#) [Author and Title](#)

**Hantouche C, Williamson B, Valinsky WC, Solomon J, Shrier A, Young JC (2017) Bag1 Co-chaperone Promotes TRC8 E3 Ligase-dependent Degradation of Misfolded Human Ether a Go-Go-related Gene (hERG) Potassium Channels. J Biol Chem 292: 2287–2300**

Pubmed: [Author and Title](#)

Google Scholar: [Author Only](#) [Title Only](#) [Author and Title](#)

**Hoang TM, Moghaddam L, Williams B, Khanna H, Dale J, Mundree SG (2015) Development of salinity tolerance in rice by constitutive-overexpression of genes involved in the regulation of programmed cell death. Front Plant Sci 6: 175**

Pubmed: [Author and Title](#)

Google Scholar: [Author Only](#) [Title Only](#) [Author and Title](#)

**Honsbein A, Blatt MR, Grefen C (2011) A molecular framework for coupling cellular volume and osmotic solute transport control. J Exp Bot 62: 2363–2370**

Pubmed: [Author and Title](#)

Google Scholar: [Author Only](#) [Title Only](#) [Author and Title](#)

**Hurst AC, Meckel T, Tayefeh S, Thiel G, Homann U (2004) Trafficking of the plant potassium inward rectifier KAT1 in guard cell protoplasts of *Vicia faba*. Plant J 37: 391–397**

Pubmed: [Author and Title](#)

Google Scholar: [Author Only](#) [Title Only](#) [Author and Title](#)

**Ivashikina N, Becker D, Ache P, Meyerhoff O, Felle HH, Hedrich R (2001) K(+) channel profile and electrical properties of *Arabidopsis* root hairs. FEBS Lett 508: 463–469**

Pubmed: [Author and Title](#)

Google Scholar: [Author Only](#) [Title Only](#) [Author and Title](#)

**Jeanguenin L, Alcon C, Duby G, Boeglín M, Chérel I, Gaillard I, Zimmermann S, Sentenac H, Véry AA (2011) AtKC1 is a general modulator of *Arabidopsis* inward Shaker channel activity. Plant J 67: 570–582**

by www.plantphysiol.org  
Copyright © 2019 American Society of Plant Biologists. All rights reserved.

- Pubmed: [Author and Title](#)  
Google Scholar: [Author Only Title Only Author and Title](#)
- Jiang Y, Lee A, Chen J, Ruta V, Cadene M, Chait BT, MacKinnon R (2003) X-ray structure of a voltage-dependent K<sup>+</sup> channel. *Nature* 423: 33–41**  
Pubmed: [Author and Title](#)  
Google Scholar: [Author Only Title Only Author and Title](#)
- Jones HG (1999) Use of thermography for quantitative studies of spatial and temporal variation of stomatal conductance over leaf surfaces. *Plant, Cell Environ* 22: 1043–1055**  
Pubmed: [Author and Title](#)  
Google Scholar: [Author Only Title Only Author and Title](#)
- Kabbage M, Dickman MB (2008) The BAG proteins: A ubiquitous family of chaperone regulators. *Cell Mol Life Sci* 65: 1390–1402**  
Pubmed: [Author and Title](#)  
Google Scholar: [Author Only Title Only Author and Title](#)
- Kabbage M, Kessens R, Dickman MB (2016) A plant Bcl-2-associated athanogene is proteolytically activated to confer fungal resistance. *Microb Cell* 3: 224–226**  
Pubmed: [Author and Title](#)  
Google Scholar: [Author Only Title Only Author and Title](#)
- Knapp RT, Wong MJH, Kollmannsberger LK, Gassen NC, Kretzschmar A, Zschocke J, Hafner K, Young JC, Rein T (2014) Hsp70 cochaperones HspBP1 and BAG-1M differentially regulate steroid hormone receptor function. *PLoS One* 9: doi:10.1371/journal.pone.0085415**  
Pubmed: [Author and Title](#)  
Google Scholar: [Author Only Title Only Author and Title](#)
- Langhans M, Meckel T, Kress A, Lerich A, Robinson DG (2012) ERES (ER exit sites) and the “Secretory Unit Concept.” *J Microsc* 247: 48–59**
- Lawson T, Blatt MR (2014) Stomatal size, speed, and responsiveness impact on photosynthesis and water use efficiency. *Plant Physiol* 164: 1556–1570**  
Pubmed: [Author and Title](#)  
Google Scholar: [Author Only Title Only Author and Title](#)
- Lebaudy A, Pascaud F, Véry AA, Alcon C, Dreyer I, Thibaud JB, Lacombe B (2010) Preferential KAT1-KAT2 heteromerization determines inward K<sup>+</sup> current properties in Arabidopsis guard cells. *J Biol Chem* 285: 6265–6274**  
Pubmed: [Author and Title](#)  
Google Scholar: [Author Only Title Only Author and Title](#)
- Lebaudy A, Vavasseur A, Hosy E, Dreyer I, Leonhardt N, Thibaud JB, Véry AA, Simonneau T, Sentenac H (2008) Plant adaptation to fluctuating environment and biomass production are strongly dependent on guard cell potassium channels. *Proc Natl Acad Sci U S A* 105: 5271–5276**  
Pubmed: [Author and Title](#)  
Google Scholar: [Author Only Title Only Author and Title](#)
- Lee DW, Kim SJ, Oh YJ, Choi B, Lee J, Hwang I (2016) Arabidopsis BAG1 Functions as a Cofactor in Hsc70-Mediated Proteasomal Degradation of Unimported Plastid Proteins. *Mol Plant* 9: 1428–1431**  
Pubmed: [Author and Title](#)  
Google Scholar: [Author Only Title Only Author and Title](#)
- Lefoulon C, Waghmare S, Karnik R, Blatt MR (2018) Gating control and K. *Plant Cell Env* 41: 2668–2677**  
Pubmed: [Author and Title](#)  
Google Scholar: [Author Only Title Only Author and Title](#)
- Li K, Jiang Q, Bai X, Yang YF, Ruan MY, Cai SQ (2017) Tetrameric Assembly of K<sup>+</sup> Channels Requires ER-Located Chaperone Proteins. *Mol Cell* 65: 52–65**  
Pubmed: [Author and Title](#)  
Google Scholar: [Author Only Title Only Author and Title](#)
- Long SB, Campbell EB, Mackinnon R (2005) Crystal structure of a mammalian voltage-dependent Shaker family K<sup>+</sup> channel. *Science* (80- ) 309: 897–903**  
Pubmed: [Author and Title](#)  
Google Scholar: [Author Only Title Only Author and Title](#)
- Mäser P, Thomine S, Schroeder JI, Ward JM, Hirschi K, Sze H, Talke IN, Amtmann A, Maathuis FJ, Sanders D, et al (2001) Phylogenetic relationships within cation transporter families of Arabidopsis. *Plant Physiol* 126: 1646–1667**  
Pubmed: [Author and Title](#)  
Google Scholar: [Author Only Title Only Author and Title](#)
- Matheson LA, Hanton SL, Brandizzi F (2006) Traffic between the plant endoplasmic reticulum and Golgi apparatus: to the Golgi and beyond. *Curr Opin Plant Biol* 9: 601–609**  
Pubmed: [Author and Title](#)  
Google Scholar: [Author Only Title Only Author and Title](#)

Meckel T, Hurst AC, Thiel G, Homann U (2004) Endocytosis against high turgor: intact guard cells of *Vicia faba* constitutively endocytose fluorescently labelled plasma membrane and GFP-tagged K-channel KAT1. *Plant J* 39: 182–193

Pubmed: [Author and Title](#)

Google Scholar: [Author Only](#) [Title Only](#) [Author and Title](#)

Merlot S, Mustilli AC, Genty B, North H, Lefebvre V, Sotta B, Vavasseur A, Giraudat J (2002) Use of infrared thermal imaging to isolate *Arabidopsis* mutants defective in stomatal regulation. *Plant J* 30: 601–609

Pubmed: [Author and Title](#)

Google Scholar: [Author Only](#) [Title Only](#) [Author and Title](#)

Mumberg D, Müller R, Funk M (1994) Regulatable promoters of *Saccharomyces cerevisiae*: comparison of transcriptional activity and their use for heterologous expression. *Nucleic Acids Res* 22: 5767–5768

Pubmed: [Author and Title](#)

Google Scholar: [Author Only](#) [Title Only](#) [Author and Title](#)

Nakamura RL, McKendree WL, Hirsch RE, Sedbrook JC, Gaber RF, Sussman MR (1995) Expression of an *Arabidopsis* potassium channel gene in guard cells. *Plant Physiol* 109: 371–374

Pubmed: [Author and Title](#)

Google Scholar: [Author Only](#) [Title Only](#) [Author and Title](#)

Navarrete C, Petrezselyova S, Barreto L, Martinez JL, Zahradka J, Arino J, Sychrova H, Ramos J (2010) Lack of main K plus uptake systems in *Saccharomyces cerevisiae* cells affects yeast performance in both potassium-sufficient and potassium-limiting conditions. *FEMS Yeast Res* 10: 508–517

Pubmed: [Author and Title](#)

Google Scholar: [Author Only](#) [Title Only](#) [Author and Title](#)

Obrdlik P, El-Bakkoury M, Hamacher T, Cappellaro C, Vilarino C, Fleischer C, Ellerbrok H, Kamuzinzi R, Ledent V, Blaudez D, et al (2004) K+ channel interactions detected by a genetic system optimized for systematic studies of membrane protein interactions. *Proc Natl Acad Sci* 101: 12242–7

Pubmed: [Author and Title](#)

Google Scholar: [Author Only](#) [Title Only](#) [Author and Title](#)

Pardo JM, Quintero FJ (2002) Plants and sodium ions: keeping company with the enemy. *Genome Biol* 3: doi:10.1186/gb-2002-3-6-reviews1017

Pubmed: [Author and Title](#)

Google Scholar: [Author Only](#) [Title Only](#) [Author and Title](#)

Paumi CM, Menendez J, Arnoldo A, Engels K, Iyer KR, Thaminy S, Georgiev O, Barral Y, Michaelis S, Stagljar I (2007) Mapping protein-protein interactions for the yeast ABC transporter Ycf1p by integrated split-ubiquitin membrane yeast two-hybrid analysis. *Mol Cell* 26: 15–25

Pubmed: [Author and Title](#)

Google Scholar: [Author Only](#) [Title Only](#) [Author and Title](#)

Pilot G, Pratelli R, Gaymard F, Meyer Y, Sentenac H (2003) Five-group distribution of the Shaker-like K+ channel family in higher plants. *J Mol Evol* 56: 418–434

Pubmed: [Author and Title](#)

Google Scholar: [Author Only](#) [Title Only](#) [Author and Title](#)

Planes MD, Niñoles R, Rubio L, Bissoli G, Bueso E, García-Sánchez MJ, Alejandro S, Gonzalez-Guzmán M, Hedrich R, Rodriguez PL, et al (2015) A mechanism of growth inhibition by abscisic acid in germinating seeds of *Arabidopsis thaliana* based on inhibition of plasma membrane H+-ATPase and decreased cytosolic pH, K+, and anions. *J Exp Bot* 66: 813–825

Pubmed: [Author and Title](#)

Google Scholar: [Author Only](#) [Title Only](#) [Author and Title](#)

Prokhnovsky AI, Peremyslov V V., Dolja V V. (2005) Actin Cytoskeleton Is Involved in Targeting of a Viral Hsp70 Homolog to the Cell Periphery. *J Virol* 79: 14421–14428

Pubmed: [Author and Title](#)

Google Scholar: [Author Only](#) [Title Only](#) [Author and Title](#)

Rodríguez-Navarro A (2000) Potassium transport in fungi and plants. *Biochim Biophys Acta* 1469: 1–30

Pubmed: [Author and Title](#)

Google Scholar: [Author Only](#) [Title Only](#) [Author and Title](#)

Ronzier E, Corratgé-Faillie C, Sanchez F, Prado K, Brière C, Leonhardt N, Thibaud JB, Xiong TC (2014) CPK13, a noncanonical Ca2+-dependent protein kinase, specifically inhibits KAT2 and KAT1 shaker K+ channels and reduces stomatal opening. *Plant Physiol* 166: 314–326

Pubmed: [Author and Title](#)

Google Scholar: [Author Only](#) [Title Only](#) [Author and Title](#)

Saponaro A, Porro A, Chaves-Sanjuan A, Nardini M, Rauh O, Thiel G, Moroni A (2017) Fusaric acid Activates KAT1 Channels by Stabilizing Their Interaction with 14-3-3 Proteins. *Plant Cell* 29: 2570–2580

Pubmed: [Author and Title](#)

Google Scholar: [Author Only](#) [Title Only](#) [Author and Title](#)

**Sarrion-Perdigones A, Vazquez-Vilar M, Palací J, Castelijnns B, Forment J, Ziarsolo P, Blanca J, Granell A, Orzaez D (2013) GoldenBraid 2.0: a comprehensive DNA assembly framework for plant synthetic biology. Plant Physiol 162: 1618–1631**

Pubmed: [Author and Title](#)

Google Scholar: [Author Only](#) [Title Only](#) [Author and Title](#)

**Sato A, Sato Y, Fukao Y, Fujiwara M, Umezawa T, Shinozaki K, Hibi T, Taniguchi M, Miyake H, Goto DB, et al (2009) Threonine at position 306 of the KAT1 potassium channel is essential for channel activity and is a target site for ABA-activated SnRK2/OST1/SnRK2.6 protein kinase. Biochem J 424: 439–448**

Pubmed: [Author and Title](#)

Google Scholar: [Author Only](#) [Title Only](#) [Author and Title](#)

**Schachtman DP, Schroeder JI, Lucas WJ, Anderson JA, Gaber RF (1992) Expression of an inward-rectifying potassium channel by the Arabidopsis KAT1 cDNA. Science (80- ) 258: 1654–1658**

Pubmed: [Author and Title](#)

Google Scholar: [Author Only](#) [Title Only](#) [Author and Title](#)

**Sessions A, Burke E, Presting G, Aux G, McElver J, Patton D, Dietrich B, Ho P, Bacwaden J, Ko C, et al (2002) A high-throughput Arabidopsis reverse genetics system. Plant Cell 14: 2985–2994**

Pubmed: [Author and Title](#)

Google Scholar: [Author Only](#) [Title Only](#) [Author and Title](#)

**Sieben C, Mikosch M, Brandizzi F, Homann U (2008) Interaction of the K(+)-channel KAT1 with the coat protein complex II coat component Sec24 depends on a di-acidic endoplasmic reticulum export motif. Plant J 56: 997–1006**

Pubmed: [Author and Title](#)

Google Scholar: [Author Only](#) [Title Only](#) [Author and Title](#)

**Sottocornola B, Gazzarrini S, Olivari C, Romani G, Valbuzzi P, Thiel G, Moroni A (2008) 14-3-3 proteins regulate the potassium channel KAT1 by dual modes. Plant Biol 10: 231–236**

Pubmed: [Author and Title](#)

Google Scholar: [Author Only](#) [Title Only](#) [Author and Title](#)

**Sottocornola B, Visconti S, Orsi S, Gazzarrini S, Giacometti S, Olivari C, Camoni L, Aducci P, Marra M, Abenavoli A, et al (2006) The potassium channel KAT1 is activated by plant and animal 14-3-3 proteins. J Biol Chem 281: 35735–35741**

Pubmed: [Author and Title](#)

Google Scholar: [Author Only](#) [Title Only](#) [Author and Title](#)

**Sutter JU, Campanoni P, Tyrrell M, Blatt MR (2006) Selective mobility and sensitivity to SNAREs is exhibited by the Arabidopsis KAT1 K+ channel at the plasma membrane. Plant Cell 18: 935–954**

Pubmed: [Author and Title](#)

Google Scholar: [Author Only](#) [Title Only](#) [Author and Title](#)

**Sutter JU, Sieben C, Hartel A, Eisenach C, Thiel G, Blatt MR (2007) Abscisic acid triggers the endocytosis of the arabidopsis KAT1 K+ channel and its recycling to the plasma membrane. Curr Biol 17: 1396–1402**

Pubmed: [Author and Title](#)

Google Scholar: [Author Only](#) [Title Only](#) [Author and Title](#)

**Szyroki A, Ivashikina N, Dietrich P, Roelfsema MR, Ache P, Reintanz B, Deeken R, Godde M, Felle H, Steinmeyer R, et al (2001) KAT1 is not essential for stomatal opening. Proc Natl Acad Sci U S A 98: 2917–2921**

Pubmed: [Author and Title](#)

Google Scholar: [Author Only](#) [Title Only](#) [Author and Title](#)

**Takayama S, Reed JC (2001) Molecular chaperone targeting and regulation by BAG family proteins. Nat Cell Biol 3: doi:10.1038/ncb1001-e237**

Pubmed: [Author and Title](#)

Google Scholar: [Author Only](#) [Title Only](#) [Author and Title](#)

**Véry AA, Gaymard F, Bosseux C, Sentenac H, Thibaud JB (1995) Expression of a cloned plant K+ channel in Xenopus oocytes: analysis of macroscopic currents. Plant J 7: 321–332**

Pubmed: [Author and Title](#)

Google Scholar: [Author Only](#) [Title Only](#) [Author and Title](#)

**Véry AA, Sentenac H (2003) Molecular mechanisms and regulation of K+ transport in higher plants. Annu Rev Plant Biol 54: 575–603**

Pubmed: [Author and Title](#)

Google Scholar: [Author Only](#) [Title Only](#) [Author and Title](#)

**Wang Y, Hills A, Blatt MR (2014) Systems analysis of guard cell membrane transport for enhanced stomatal dynamics and water use efficiency. Plant Physiol 164: 1593–1599**

Pubmed: [Author and Title](#)

Google Scholar: [Author Only](#) [Title Only](#) [Author and Title](#)

**Wang Y, Holroyd G, Hetherington AM, Ng CKY (2004) Seeing "cool" and "hot" - Infrared thermography as a tool for non-invasive, high-throughput screening of Arabidopsis guard cell signalling mutants. J Exp Bot 55: 1187–1193**

Pubmed: [Author and Title](#)

Google Scholar: [Author Only](#) [Title Only](#) [Author and Title](#)

**Williams B, Kabbage M, Britt R, Dickman MB (2010) AtBAG7, an Arabidopsis Bcl-2-associated athanogene, resides in the endoplasmic reticulum and is involved in the unfolded protein response. Proc Natl Acad Sci 107: 6088–6093**

Pubmed: [Author and Title](#)

Google Scholar: [Author Only](#) [Title Only](#) [Author and Title](#)

**Winter D, Vinegar B, Nahal H, Ammar R, Wilson G V, Provart NJ (2007) An "Electronic Fluorescent Pictograph" browser for exploring and analyzing large-scale biological data sets. PLoS One 2: e718**

Pubmed: [Author and Title](#)

Google Scholar: [Author Only](#) [Title Only](#) [Author and Title](#)

**Wu HY, Liu KH, Wang YC, Wu JF, Chiu WL, Chen CY, Wu SH, Sheen J, Lai EM (2014) AGROBEST: an efficient Agrobacterium-mediated transient expression method for versatile gene function analyses in Arabidopsis seedlings. Plant Methods 10: 19**

Pubmed: [Author and Title](#)

Google Scholar: [Author Only](#) [Title Only](#) [Author and Title](#)

**Xicluna J, Lacombe B, Dreyer I, Alcon C, Jeanguenin L, Sentenac H, Thibaud JB, Chérel I (2007) Increased functional diversity of plant K<sup>+</sup> channels by preferential heteromerization of the shaker-like subunits AKT2 and KAT2. J Biol Chem 282: 486–494**

Pubmed: [Author and Title](#)

Google Scholar: [Author Only](#) [Title Only](#) [Author and Title](#)

**Yan A, Wu E, Lennarz WJ (2005) Studies of yeast oligosaccharyl transferase subunits using the split-ubiquitin system: topological features and in vivo interactions. Proc Natl Acad Sci U S A 102: 7121–7126**

Pubmed: [Author and Title](#)

Google Scholar: [Author Only](#) [Title Only](#) [Author and Title](#)

**Yang Y, Costa A, Leonhardt N, Siegel RS, Schroeder JI (2008) Isolation of a strong Arabidopsis guard cell promoter and its potential as a research tool. Plant Methods 4: 6**

Pubmed: [Author and Title](#)

Google Scholar: [Author Only](#) [Title Only](#) [Author and Title](#)

**Young JC (2014) The role of the cytosolic HSP70 chaperone system in diseases caused by misfolding and aberrant trafficking of ion channels. Dis Model Mech 7: 319–329**

Pubmed: [Author and Title](#)

Google Scholar: [Author Only](#) [Title Only](#) [Author and Title](#)

**Zhang B, Karnik R, Waghmare S, Donald N, Blatt MR (2017) VAMP721 Conformations Unmask an Extended Motif for K<sup>+</sup> Channel Binding and Gating Control. Plant Physiol 173: 536–551**

Pubmed: [Author and Title](#)

Google Scholar: [Author Only](#) [Title Only](#) [Author and Title](#)

**Zhang B, Karnik R, Wang Y, Wallmeroth N, Blatt MR, Grefen C (2015) The Arabidopsis R-SNARE VAMP721 Interacts with KAT1 and KC1 K<sup>+</sup> Channels to Moderate K<sup>+</sup> Current at the Plasma Membrane. Plant Cell 27: 1697–1717**

Pubmed: [Author and Title](#)

Google Scholar: [Author Only](#) [Title Only](#) [Author and Title](#)